2024

Kattegat Offshore Wind Farm and Export Cable Route Geoarchaeological Analysis

Daniel Dalicsek, Peter Moe Astrup and Kristine R. Fischer

Marinarkæologi Vestdanmark (MAV)

15-12-2024

Resume

Marinarkæologi Vestdanmark (MAV) har udarbejdet nærværende geoarkæologiske analyse for Energinet med henblik på at kortlægge potentielle kulturhistoriske interesser på havbunden for den planlagte havvindmøllepark Kattegat og kabelruten til ilandføring. Den geoarkæologiske rapport vurderer risici for fortidsminder fra stenalderen i forbindelse med anlægsarbejdet. Dette gøres ved at genskabe stenalderslandskaberne som de så ud inden de blev oversvømmet og udpege de områder som vurderes at have særligt stort arkæologisk potentiale (såkaldte arkæologiske hotspots). Det er ligeledes blevet identificeret hvor disse hotspots er tilgængelige (bevaret) og hvor de i dag er borteroderet og eller ikke berøres af anlægsarbejdet.

Rapporten har også til formål at identificere de vrag og rester af skibslaster der er i området. I analysen er der derfor også blevet udpeget anomalier på baggrund af de af Energinet leverede geofysiske data. Vurderingerne og udpegningerne er mere konkret baseret på side-scan sonar data, magnetometer data, multibeam data og diverse kulturhistoriske registre.

Der er i alt udpeget 2451 anomalier i projektområdet. Af disse tilskrives 77 CONF 1, 113 CONF 2, 782 CONF 3 og 1479 CONF 4 og CONF 5 (formentlig moderne MMOs eller geologiske objekter). Blandt anomalierne er flere ankre og en anomali som tolkes som et muligt historisk skibsvrag.

Det er Slots- og Kulturstyrelsen (SLKS), der har til opgave at beslutte hvilke af de udpegede anomalier, som skal besigtiges og eventuelt friholdes som et led i en forundersøgelse. Det er ligeledes SLKSs rolle at fastsætte eventuelle friholdelseszoner omkring vrag og anomalier mm. Nærværende rapport kan således betragtes som en museal anbefaling hvorfra SLKS kan træffe deres afgørelse.

Abstract

On behalf of Energinet, the Maritime Archaeology of Western Denmark (MAV) has carried out the below desk-based geoarchaeological study of the project area ahead of the construction of the offshore wind park Kattegat and the related Export Cable Route.

The Stone Age potential has been assessed, in the whole project area, as part of the analysis. The analysis was conducted by recreating the Stone Age landscape as it was before it was inundated and by identification of the areas which are considered to have particularly high archaeological potential (so-called hotspots). Secondly it was identified where these hotspots are accessible (preserved) and where they are now eroded away or considered not to be affected by the construction work.

In the analysis, anomalies have been identified on the basis of the geophysical data supplied by Energinet. The assessments and designations are based on side-scan sonar data, magnetometer data and multibeam data, correlated to existing archival data. There are 982 SSS anomalies detected in the OWF project area and 1439 anomalies in the ECR area. Of these, 77 are designated CONF 1, 113 CONF 2, 782 CONF 3 and 1479 CONF 4 or CONF 5 (most likely modern MMOs or geological features). Among the anomalies are several anchors and one anomaly interpreted as a possible shipwreck.

It is the responsibility of the Agency for Culture and Palaces (SLKS) to decide which of the above-mentioned anomalies should be inspected and possibly protected as part of an archaeological pre-survey. It is also the role of SLKS to define exclusion zones around wrecks and anomalies etc.

Cover picture 1 Kattegat OWF and ECR on a 1773 nautical chart

Table of Contents

List of figures

List of tables

List of abbreviations and definitions

BC	Before Christ
BH	Borehole
BSU	Base Seismic Unit
cal	Calibrated
CE	Current Events
CONF	Confidence (relating to archaeology)
CPT	Cone Penetration Test
DKM	De Kulturhistoriske Museer i Holstebro
ECR	Export Cable Route
EfS	'Efterretninger for Søfarende', Notices to Mariners.
EI	Energy Island
EOD	Explosive Ordnance Disposal
FFM	Fund og Fortidsminder, the Danish Sites and Monuments Record
GEUS	Geological Survey of Denmark and Greenland
GIS	Geographic Information System
GRT	Gross Register Tons
HF	High Frequency
LF	Low Frequency
LOA	Length over all
MAG	Magnetometer
MAJ	Marinarkæologi Jylland (predecessor to MAV)
MAV	Marinarkæologi Vestdanmark
MASL	Meters Above Sea Level
MBES	Multibeam Echo Sounder
MMO	Man Made Object
MOMU	Moesgaard Museum
NKM	Nordjyllands Kystmuseum
nT	Nanotesla
oa	Over all
OWF	Offshore Wind Farm
P2P	Peak to peak
pUXO	Potential UXO
ROV	Remotely Operated Vehicle
SBP	Sub-Bottom Profiler
SLIP	Sea Level Index Point
SLKS	Slots- og Kulturstyrelsen
SOW	Scope Of Work
SSS	Side Scan Sonar
uncal	Uncalibrated
UXO	Unexploded Ordnance
WWI	World War One
WWII	World War Two

1. Introduction

1.1. Project background

The government and a broad majority of the parliamentary parties decided in May 2023 that an offshore wind farm should be offered in the area of Kattegat. The OWF Kattegat will be placed 15-30km away from the eastern coast of the Djursland peninsula. The offshore infrastructure will consist (among others) of offshore wind turbines, transformer platforms and inter-array cables, whereas the onshore infrastructure will be made up of ground-based cables, high voltage sub-stations and possible grid upgrades and extensions.

Figure 1 Conceptual illustration of the Kattegat OWF project area Source: Energinet

Energinet had been tasked with carrying out the preliminary studies and impact assessments for the offshore infrastructure, as well as to prepare the onshore grid connections. This work has already started. The eventual contractor(s) and operator(s) of the OWF will be decided through the Danish Energy Agency's tendering process.

The construction, operation and decommissioning of the OWF and the ECR may impact maritime archaeological find locations. Activities such as anchoring and jacking-up of vessels used during construction work can damage cultural heritage in the affected areas. The work could potentially endanger maritime archaeological objects such as shipwrecks, wreckage and Stone Age find locations.

Energinet has therefore asked the maritime archaeological museums in the collaboration Marinarkæologi Vestdanmark (MAV) to carry out a geoarchaeological analysis (see 17/03563-1 Best Practice) of the proposed construction area of Kattegat to evaluate the extent to which this project will affect objects and areas protected by Section 28 of the Danish Museum Act. The work seeks to determine the presence of cultural heritage, such as traces of human activity from the Stone Age or cultural-historical objects such as shipwrecks.

1.2. Administrative and other data

The geoarchaeological analysis is carried out for Energinet. The contact person is Nicky Hein Witt. Moesgaard Museum (i.e. MAV) is responsible for the archaeology in the project area (Figure 2).

It was decided at the MERE HAVVIND 2030 MARINARKÆOLOGI KICK OFF meeting, held on the 1st of February 2023, that the responsibility for the geoarchaeological analysis lies with Moesgaard Museum. The contact person is Daniel Peter Dalicsek (DAD) and Peter Astrup (PMA). The responsibility for historical archaeology was transferred to Nordjyllands Kystmuseum (NJK) on the 07/03/2024. The contact person is Jan Hammer Larsen (JHL).

The wind farm operator and company responsible for construction hasn't been found yet. However, it is advised that the company selected for those tasks in the future contacts MAV as early as possible in the planning process to mitigate questions concerning maritime archaeology. The geoarchaeological analysis is archived at Moesgaard Museum under the filing number MAV2023-048 Kattegat.

This report is delivered in accordance with "AFTALE OM LEVERING AF GEOARKÆOLOGISK ANALYSE FOR MERE HAVVIND 2030 KATTEGAT" and based on the data provided by Energinet.

Table 1 Administrative and other data

Accountable museum:	Marinarkæologi Vestdanmark (MAV)
Museum contact:	Peter Moe Astrup
Report responsibility:	Peter Moe Astrup, Jan Hammer Larsen
Report finish date:	15-12-2024
Participating archaeologists:	Peter Moe Astrup and Kristine R. Fischer (MM), Jan Hammer Larsen (NKM), Daniel Dalicsek (MM)
Stone Age responsibility:	PMA og KRF
Historical archaeology responsibility:	JHL
Name of site:	Kattegat
Site and location number (FF):	400120c-1347
MAJ collaboration case no.:	MAV2023-48 Kattegat
SLKSs case no.:	
Date of approval of budget:	29-11-2023
Type of budget:	Geoarchaeological analysis
Period of investigation:	2024
Date of project description	29-11-2023
Contractor name	Energinet
Contractor address	Tonne Kjærsvej 65, 7000 Fredericia
Contractor type	Public
Contractor CVR no.	28980671
Coordinates:	X 638518.4 Y 6247798.4
Geographic coordinate system:	Euref89 UTM zone 32N
Water depth:	0-48,0 meters
Area of investigation:	147,2 km^2

1.3. Project goals

The goal of the geoarchaeological analysis is to analyse, identify, locate and map wrecks and wreckage on or buried underneath the seafloor, as well as prehistoric landscapes, meaning also locations of potential archaeological interest, such as submerged coastal zones, that could have served as prehistoric settlement sites. Furthermore, the geoarchaeological analyses has as its goal to judge the potential for preservation of possible finds and find locations.

The geoarchaeological analysis, according to best practice, follows the geological surveys and is followed by maritime archaeological surveys, if deemed necessary, in the project chronology.

1.4. Scope of work

The geoarchaeological analysis is conducted in the period March 2024 - December 2024. The deadline for the report is the 15th of December 2024. The report covers the entire planned wind farm area and cable area and includes all available data and resources.

1.4.1. Deviations from Scope of Work

The northern cable corridor, included in the earlier archaeological analysis had been cancelled and is not investigated for this geoarchaeological analysis. The scope of work has been changed from separate reports for the OWF area and the ECR to one combined geoarchaeological report.

1.5. Reference documents

Document	Title	Author
GEUS 2023/33 Danish Energy Agency ID 1301	Screening of seabed geological conditions for the offshore wind farm area Kattegat and the adjacent cable corridor area. Desk study for Energinet.	GEUS
MAJ2022-38 North Sea cable routes MARINE ARCHAEOLOGY: GEO-ARCHAEOLOGICAL ANALYSIS, REPORT	North Sea cable routes MARINE ARCHAEOLOGY: GEO-ARCHAEOLOGICAL ANALYSIS, REPORT	MAV
Danish Energy Agency ID 1303 BE5376H-711-02-RR	Geophysical and Geological Survey Report For Kattegat	GEOxyz
MAJ2023-48 Kattegat Havvindmøllepark og kabelruter Arkæologisk analyse Danish Energy Agency ID 1302	Kattegat Havvindmøllepark og kabelruter Arkæologisk analyse	MAV
17-03563-1 Best Practice - Marinarkæologi 8026239_1_1		SLKS/ENERGINET
17-03563-2 Best Practice - Bilag 1 - Samarbejdsskema 8026240_1_1		SLKS/ENERGINET
17-03563-3 Best Practice - Bilag 2 - Geoarkæologi 8026241_1_1		SLKS/ENERGINET
23/08609-2	AFTALE OM LEVERING AF GEOARKÆOLOGISK ANALYSE FOR MERE HAVVIND 2030 KATTEGAT	ENERGINET
ACTION LIST.xlsx		ENERGINET
SN2023_027_SURVEYS_POL_Kattegat_II.shp		ENERGINET
SN2023_027_KP_ROUTE_LIN_KAttegat_II		ENERGINET
DOW2030_POL_Kattegat_II		ENERGINET

2. Submerged Stone Age potential

2.1. Registered cultural heritage artefacts

As a part of an archaeological test survey for the establishment of a cable route from the Anholt OWF to the island of Anholt in 2014, a piece of worked flint was found at a depth of approx. 12 m. The small piece of flint was found by archaeologist in material that was sucked into the ship (the accurate position of the find spot is E645437 N6281507). Another test survey was undertaken near Hjelm (c. 25 km southwest of the Kattegat OWF area) where 20 positions were examined for archaeological material with a mechanical excavator in 2024. No finds were proven in this survey that is registered with project number MAJ2021-65 Moselgrund.

2.2. topographic potential for traces of early Stone Age activity

A thick layer of ice covered large parts of Denmark during the Late Pleistocene. But ca. 20,000-18,000 years ago the ice began to retreat, partly because of melting due to increasing temperatures and partly because of glaciers calving icebergs into the sea. Enormous quantities of glacial meltwater were released into the world's oceans throughout the Mesolithic period that ended about 6,000 years ago. Studies have shown that global sea levels have risen 130m since the Late Glacial Maximum ca. 20,000-18,000 years ago (Fairbanks 1989; Lambeck et al. 2014). Peat layers described in the Kattegat core logs and submerged Stone age sites near Djursland are also evidence of sea-levels that were significantly lower than now. These sea-level changes are still not precisely determined for the Kattegat area, but from other studies (Bennike et al. 2021) it is clear that Stone Age sites will either date to the Late Palaeolithic or Early Mesolithic.

Figure 2 Schematic of cultural and natural developments in South Scandinavia in calibrated years BC. (Astrup 2018)

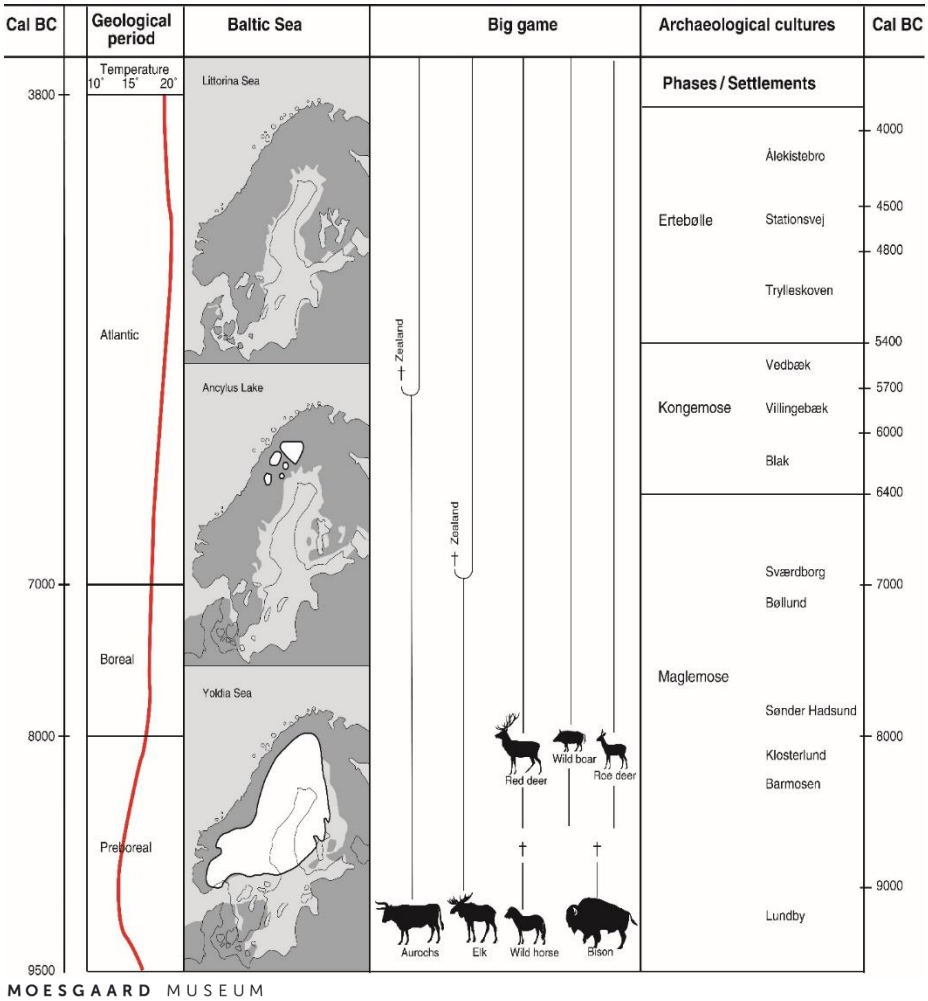

Many years of archaeological investigations have shown that Stone Age people did not randomly occupy landscapes. Rather, they chose their locations strategically based on a range of parameters in order to secure access to necessary resources, cultivate social networks, and maintain demographic viability. By reconstructing the now submerged landscapes as they appeared at various points in the past, it is possible to pinpoint areas that were better suited than others to obtain the necessary conditions for prehistoric lifestyles. Creating a detailed picture of the prehistoric landscape(s) is therefore vital to understanding where the coming construction work is at its highest risk of destroying potential archaeological localities. Evaluating an area's potential to have Stone Age settlements is typically based on topographic variables like the presence of lakes, streams, and coasts. However, in practice, different periods varied widely in their requirements for specific natural features and their accompanying resources. While most of the source material for our understanding of prehistoric hunter-gatherers in Denmark in the millennia prior to the Neolithic comes from coastal settlements, as of this writing it is unclear to what extent Late Palaeolithic and Early Mesolithic people also prioritized these areas.

In the Kattegat project area potential Stone Age settlements (coastal as well as inland) are now on (or under) the sea floor. It is precisely here, that over the past years maritime archaeology in the Danish inshore waterways has shown the potential for making major scientific advances. This is primarily due to two factors that can be characterized as "Preservation" and "Knowledge lacunae" (see below).

2.2.1. Preservation

Conditions of preservation on submerged settlements are renowned for being extremely good for organic materials such as wood and bones (see Andersen 2013). This is the result of continuously rising sea levels that inundated coastal settlements. In the process, the archaeological layers and materials were enclosed in anoxic surroundings that have remained that way to the present day. Because of the special environment in these submerged cultural layers, oxygen was not present in sufficient amounts to allow the onset of decay, creating a sort of time capsule. Previous investigations of submerged settlements from the Kongemose- and Ertebølle cultures have provided completely new insights into the types of wooden implements used in the Stone Age. This provides the example for the huge scientific potential submerged Stone Age sites in the Kattegat area could hold.

2.2.2. Knowledge lacunae

Submerged Stone Age landscapes on the sea floor represent one of the last unexplored areas in the Danish archaeological milieu. Because of this, they likely contain information that can fill some gaps in our knowledge that have remained unanswered by archaeological investigations since the recognition of the various periods of the Stone Age. It is still unknown, for example, what role coasts played in the Maglemose culture (11,500-8,400 BP), as the subsistence economy of that period is almost exclusively known from archaeological remains found at inland sites far from them. Targeted diving investigations in archaic coastal areas are therefore a prerequisite for resolving important research questions such as:

- How widespread was coastal settlement in the Late Palaeolithic and early Mesolithic cultures?
- How important a role did marine resources play in subsistence and what methods were used to collect them?
- Were coastal settlements occupied longer than those inland? Did the same people use both types of sites, or were there some groups who occupied the coast while others remained inland?

The above points serve to illustrate that there is much we still do not know about life along the coasts in the Maglemose culture. Thus, it is also a difficult task to decide where in the landscape Stone Age people settled in the Kattegat area. However, this does not change the fact that it is crucial to have as detailed an understanding of the landscape as possible, since it formed the basis of life for the people who lived in the construction area. Considering this, the next section of the report aims to step-by-step recreate a detailed picture of the now submerged cultural landscape in the project area. The goal is to be able to evaluate which areas have the greatest potential for prehistoric settlements and whether they will today still contain preserved remains. In concrete terms this means constructing a model of past sea levels and using the geophysical data to identify relevant archaic terrain.

2.3. Geological developments in the Kattegat OWF and ECR sites

The Kattegat OWF area is located around 20 km east of Grenaa. The Kattegat OWF lies along the Sorgenfrei–Tornquist Fault Zone, which is a significant fault system stretching from southern Sweden through Kattegat into northern Jutland. This fault zone has been active since the Palaeozoic era and has continued to show activity during the Quaternary due to glacio-isostatic adjustments resulting from the presence of ice sheets (Jensen et al. 2002; GEUS 2020). The fault zones main faults include the Børglum and Grenå–Helsingborg Faults both which have a distinct southeast to northwest orientation. The bedrock at the Kattegat OWF and cable route is expected to consist of Danien limestone in the southern half and Jurassic and Cretaceous sandy mudstone in the northern half (Erlström et al. 2001).

2.3.1. Quaternary geology

2.3.1.1. Pleistocene geology

Several glacial events have been documented in the Danish area. Generally, three major glaciations are recognized. The Elster glaciation (480-410 kyr BP), the Saalian glaciation (370-135 kyr BP) and the Weichselian glaciation (117-11.7 kyr BP) (e.g. Ehlers et al. 2011; Houmark-Nielsen et al. 2012; Cohen 2012). These glaciations had a significant impact on the geology and geomorphology of the Danish area. The Kattegat OWF site has been covered by ice sheets in the three major glaciations. At the Last Glacial Maximum (LGM), 22,000 years ago, the ice margin reached the Main Stationary line in central Jutland (Houmark-Nielsen et al. 2012). At that time, the Kattegat OWF area was subglacial, undergoing associated processes such as the formation of subglacial meltwater channels, glaciotectonic movements, and deposition of till. The ice sheets retreated from the Kattegat OWF area around 18,000 years BP according to Houmark-Nielsen & Kjaer (2003) (see Figure 3).

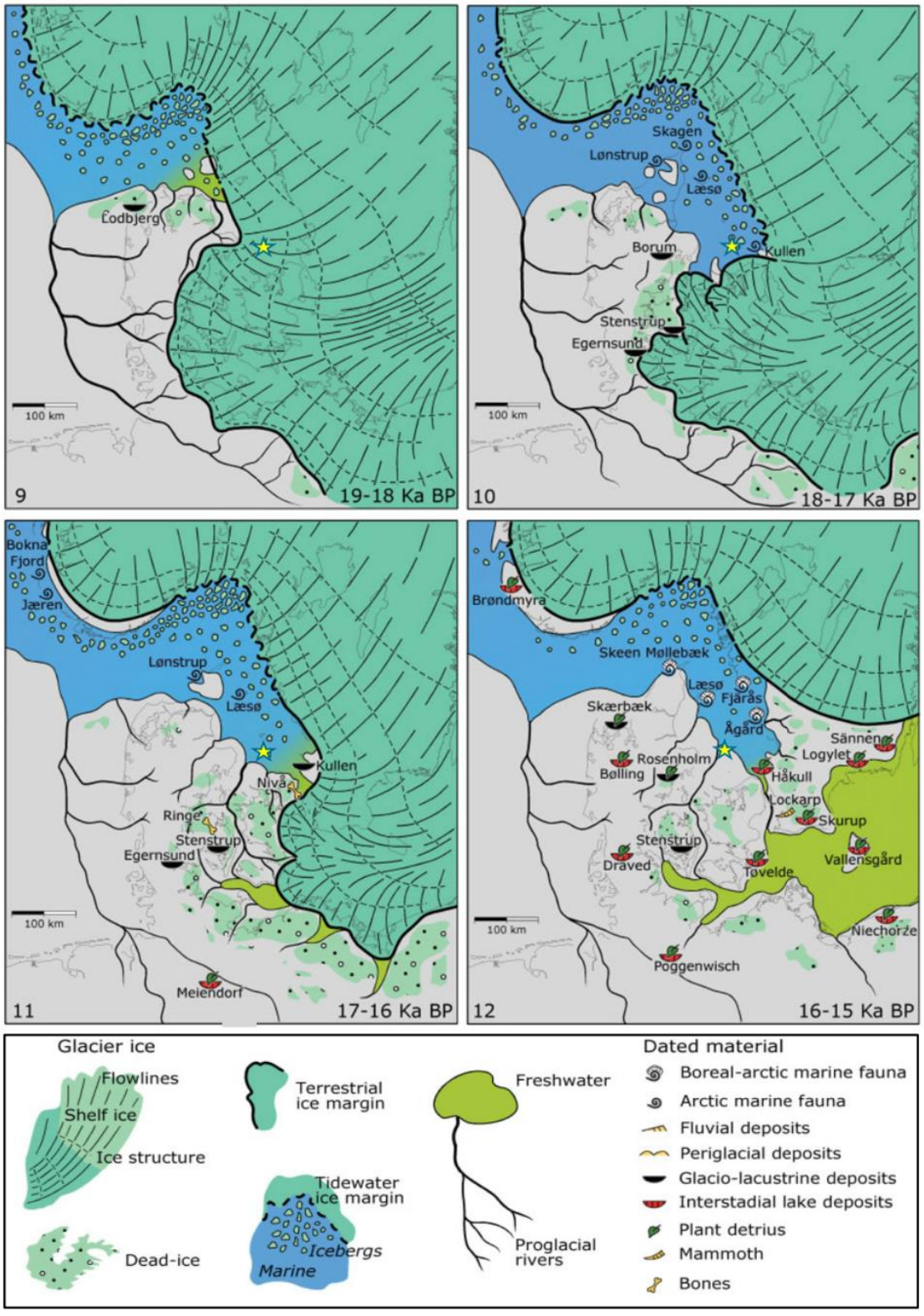

Figure 3 Reconstruction of ice movements and associated processes in the period following the Last Glacial Maximum. The ages presented are associated with uncertainties, as recent studies propose alternative timelines (e.g. Bendixen et al. (2017a)). Note that the star on the figure marks the Hesselø OWF. The Kattegat OWF is located around 20 km west of this star. Figure from Houmark-Nielsen & Kjaer (2003).

2.3.1.2. Late glacial and Holocene geology

Since the LGM, a rising temperature trend has been seen in the global climate, leading to a stepwise retreat of the Scandinavian ice sheets (see Figure 3). This retreat, combined with icebergs calving into the ocean, has contributed to a global sea level rise of approximately 130 meters (Lambeck et al. 2014). Northern Jutland, including the Kattegat area, was heavily affected by isostatic depression during the last glacial period (Richardt 1996, Astrup 2018). The ice pressed the land down into the asthenosphere, creating a lower-lying area than before. When the ice sheets retreated 18,000 years ago, the global sea level gradually rose and inundated the Kattegat area. However, due to isostatic depression, regional seawater levels were relatively high even though the eustatic sea level was still low. This resulted in the deposition of fine sediments like clay and silt (Jensen et al. 2002). Later, isostatic rebound, combined with the still-rising sea level, caused regional sea levels in the Kattegat to drop.

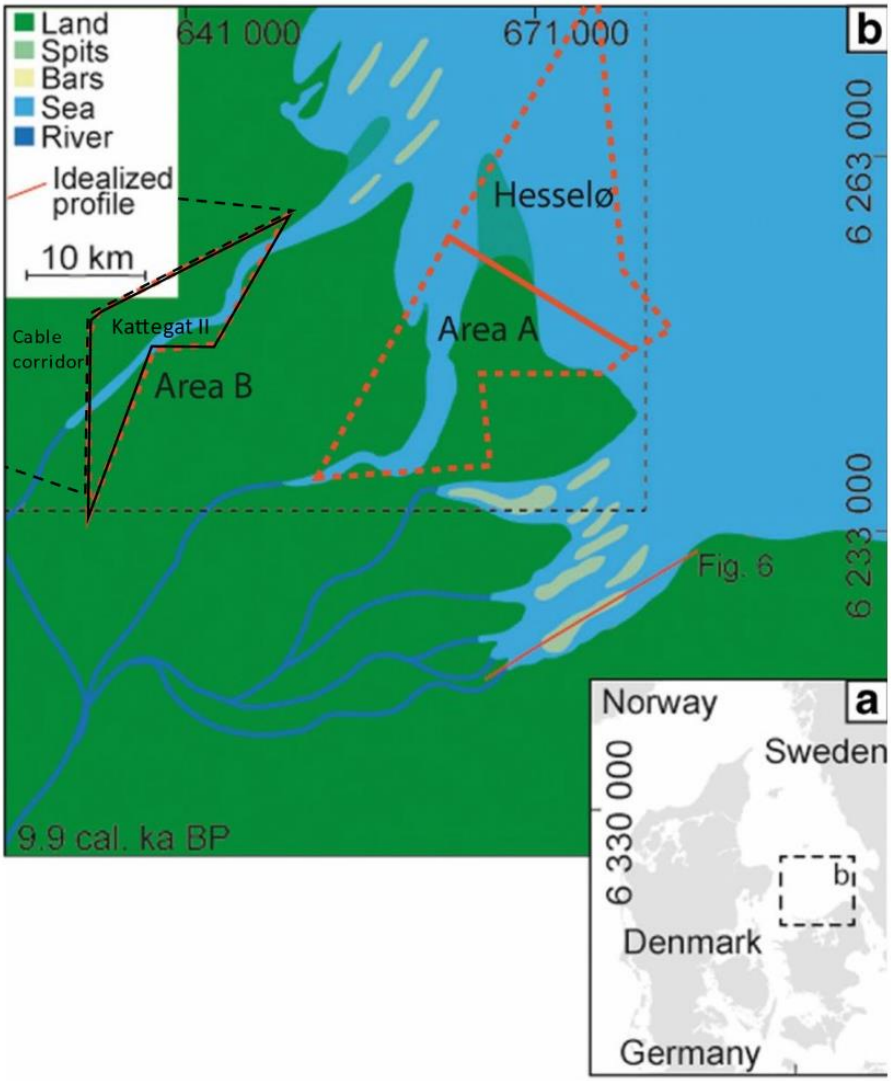

Figure 4 Environmental overview 9.9 cal ka BP for the Kattegat OWF and Hesselø OWF areas. Figure from Bendixen et al. (2017a), modified by Jensen et al. (2023).

Bendixen et al. (2017a) conducted a study in the southern Kattegat, suggesting that during the period of low sea levels around 10.3–9.2 cal. ka BP, the area functioned as an estuarine where parts of the area were dry land or coastal wetlands (see Figure 4), indicated by the presence of peat. They also found that this regression led to coastal erosion and the formation of land channels. During the estuarys existence, the Ancylus Lake drained into the Kattegat through the Dana River (paleo-Great Belt channel) (see Figure 4). The Ancylus Lake formed during the early Holocene as a result of ice sheets melting in the last glaciation. When these ice sheets melted, large quantities of freshwater filled the Ancylus Lake (Björck 1995), which occupied what is now the Baltic Sea. Initially, the basin was isolated from the ocean, forming the freshwater lake (see Figure 3), but it later drained into the Kattegat.

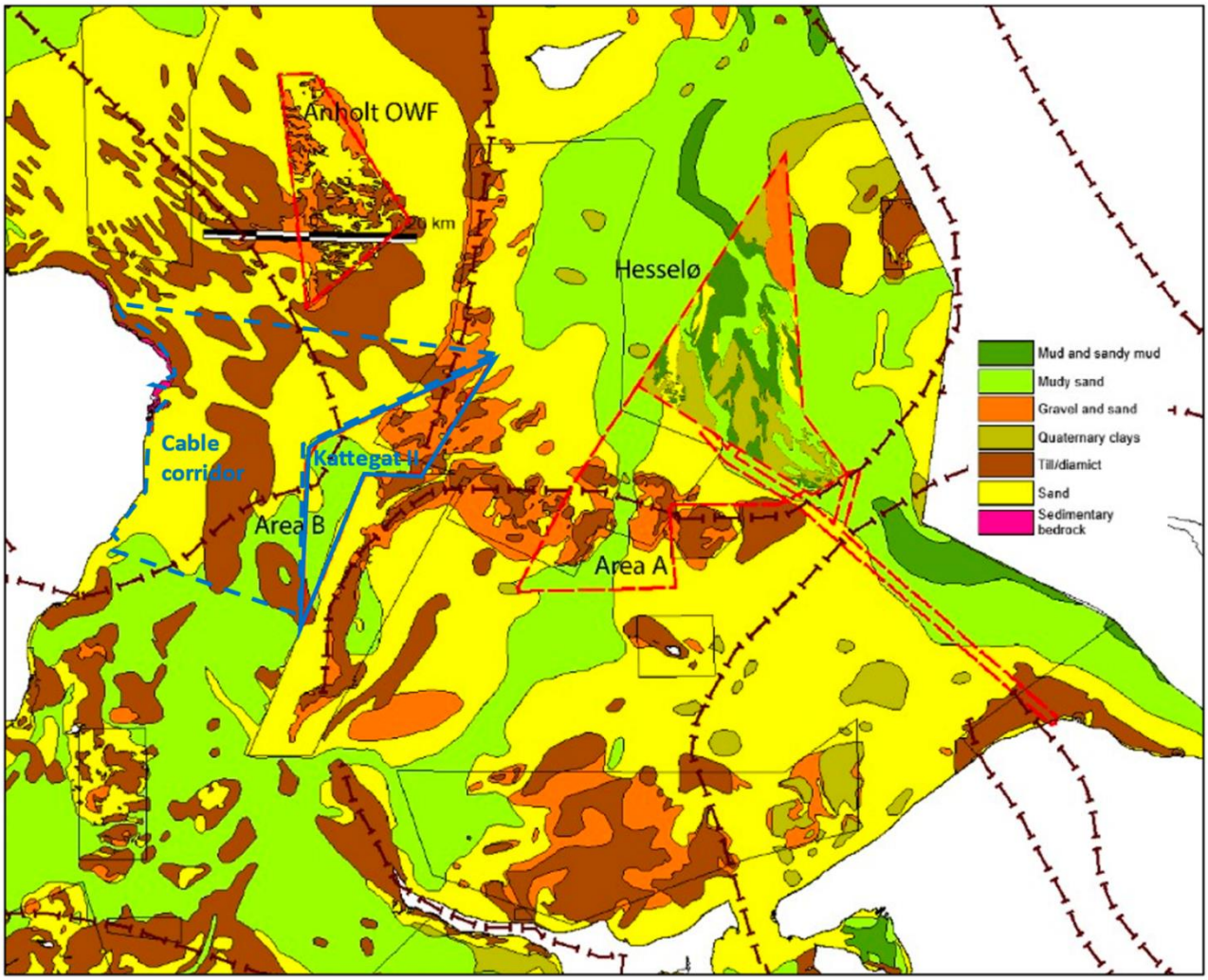

Figure 5 Lithological overview of seabed sediments from the southern Kattegat area including outlined areas of the Kattegat OWF site and belonging cable route, Anholt OWF and the Hesselø OWF site and belonging cable routes. Figure from Jensen et al. (2023).

As relative sea levels continued to rise during the Holocene, the Kattegat area was gradually flooded, pushing coastlines and related systems further inland (Jensen et al. 2002; Bendixen et al. 2017b). This led to the deposition of mud and gyttja in the deeper parts. The surface sediments in the southern half of the Kattegat OWF consist of muddy sand, while the northern surface sediments consist of sand, till and areas with gravel and sand. Similarly, the surface sediments along the cable routes also consist of these sediment types (see Figure 5). The meandering river system is still present on the seabed today as a broad, deep feature.

2.4. Borehole and vibrocore data

2.4.1. Borehole data from the Kattegat OWF site

Gardline provided different types of CPT (Cone Penetration Test) data and borehole data from the Kattegat OWF site, with descriptions that integrate data from both methods. In total, descriptions from 22 locations were included. Materials from four sediment sampling sites identified as KG_02, KG_07, KG_12, and KG_25, were dated and used as sea-level index points for the study. Borehole data went down to a depth of 7m and descriptions include interpreted soil types. The core logs from Gardline include information on sediment type and depth but does not provide estimated ages or depositional environment. In general, borehole numbering begins in the north with KG_02, increasing southward to KG_25. Borehole KG_12 and KG_25 each found sand within the top 7m. Borehole KG_02 and KG_07 contained sand and clay within the top 7m. The dated materials include a variety of sedimentary deposits, such as marine shells, often found in sand or clay matrices, as well as organic materials like wood and hazelnut/nutshells. These deposits reflect diverse depositional environments, ranging from marine to terrestrial. The radiocarbon ages span from approximately 2129 BP to 9148 BP (dates are presented in Appendix 6.3). The youngest terrestrial sample (hazelnut from KG_25) dated 8871 years BP, and the oldest marine sediment (shell from KG_12) dated 7538 years BP, suggesting that the inundation of the area happened around this time.

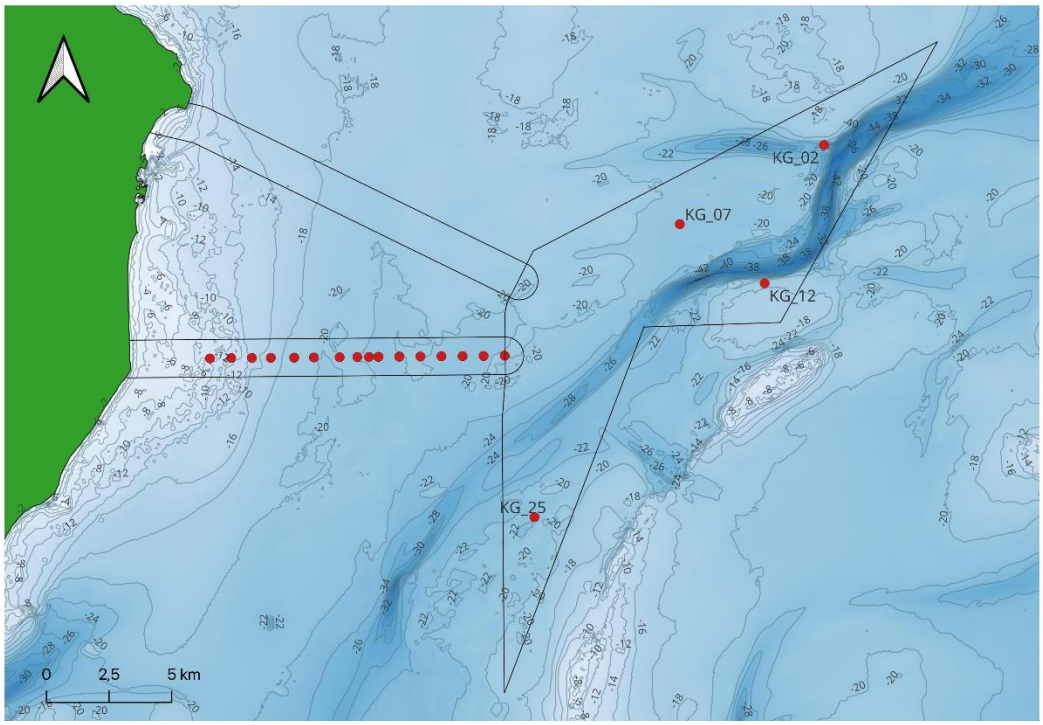

Figure 6 Boreholes used for dating material in the OWF area.

2.4.2. Vibrocore data from the Kattegat cable routes

Preliminary vibrocore logs for the Kattegat cable route were provided by GEO. These vibrocores extend offshore, with the smallest numbers being closest to the coast and vice versa (see Figure 7 below). Logs for 16 vibrocores (GT_VC_80 – GT_VC_95) were available.

The vibrocores taken along the cable routes reveal that the upper 0.1 to 3 meters typically consist of postglacial marine sand, often containing shell fragments. This layer is generally underlain by 0.2 to 2 meters of marine postglacial sand, gravel, or clay, or alternatively, by 1 to 2 meters of clayey till or 1-5 m of cretaceous meltwater sand/gravel.

Similar to the lithological overview of the southern Kattegat (Figure 5), the borehole and vibrocore records reveal an environment shaped by a complex interplay of environmental forces. These include meltwater river systems, which transported sediments and reshaped the terrain; glacial deposits from ice advances and retreats, which left layers of till and other glacial sediments; and marine deposits, marking phases of postglacial sea-level rise and changing coastal conditions. Thereby these deposits represent the transition from ice dominated landscapes to river influenced terrains and eventually a submerged marine landscape.

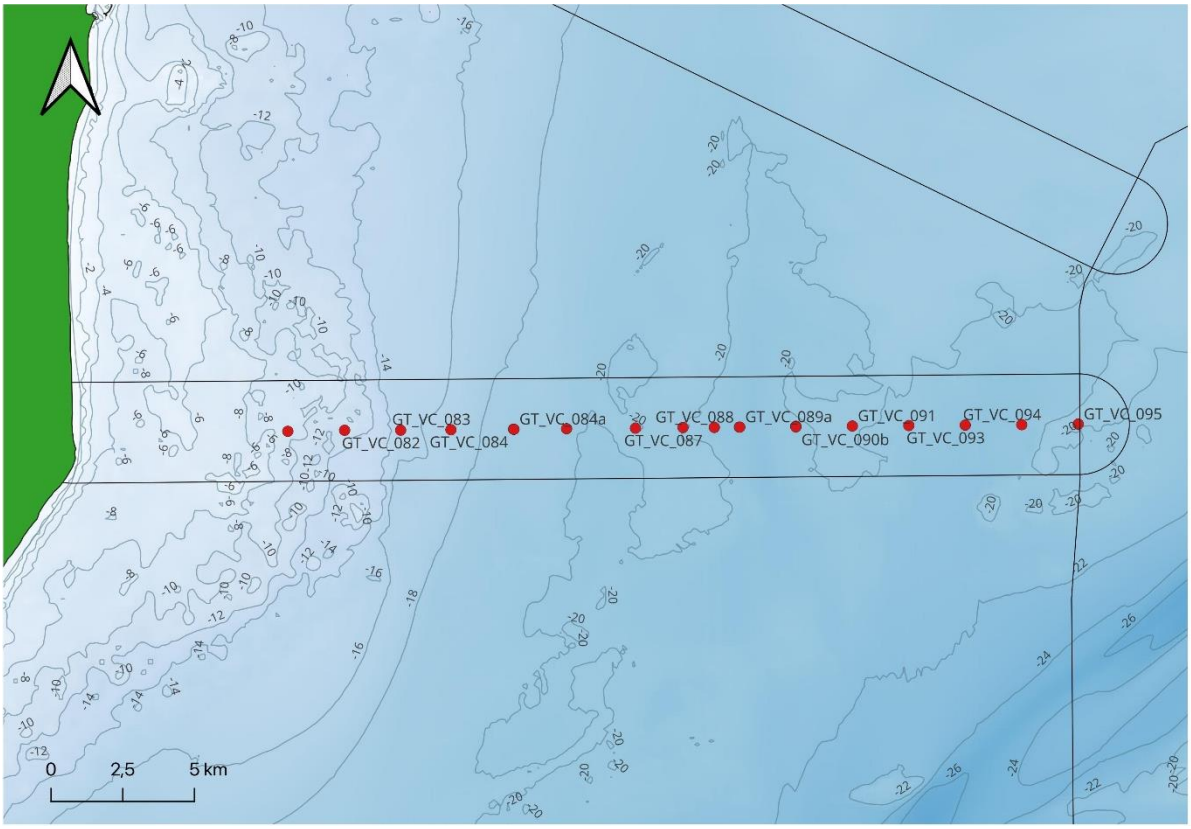

Figure 7 Vibrocore locations in the Kattegat ECR project area.

2.5. Modelling sea levels

2.5.1. Collection of data

It is vital to understand the development of the landscape in a given region to be able to identify the parts of a project area that have the greatest archaeological potential. It is by no means a simple task to reconstruct the old coastlines in the Kattegat area and an important reason for this is that the extent of glacial isostatic rebound in the project area is not yet clear. Because of differences in the rate at which land has rebounded from when it was pressed down by the glaciers, it is impossible to reconstruct archaic coastlines across larger areas simply by simulating a drop in sea-level on the modern bathymetric data. Additionally, from the Kattegat area there are so few dated samples that the relative sea level rise is difficult to determine. It will therefore be vital to develop a shoreline displacement curve based on data from the area.

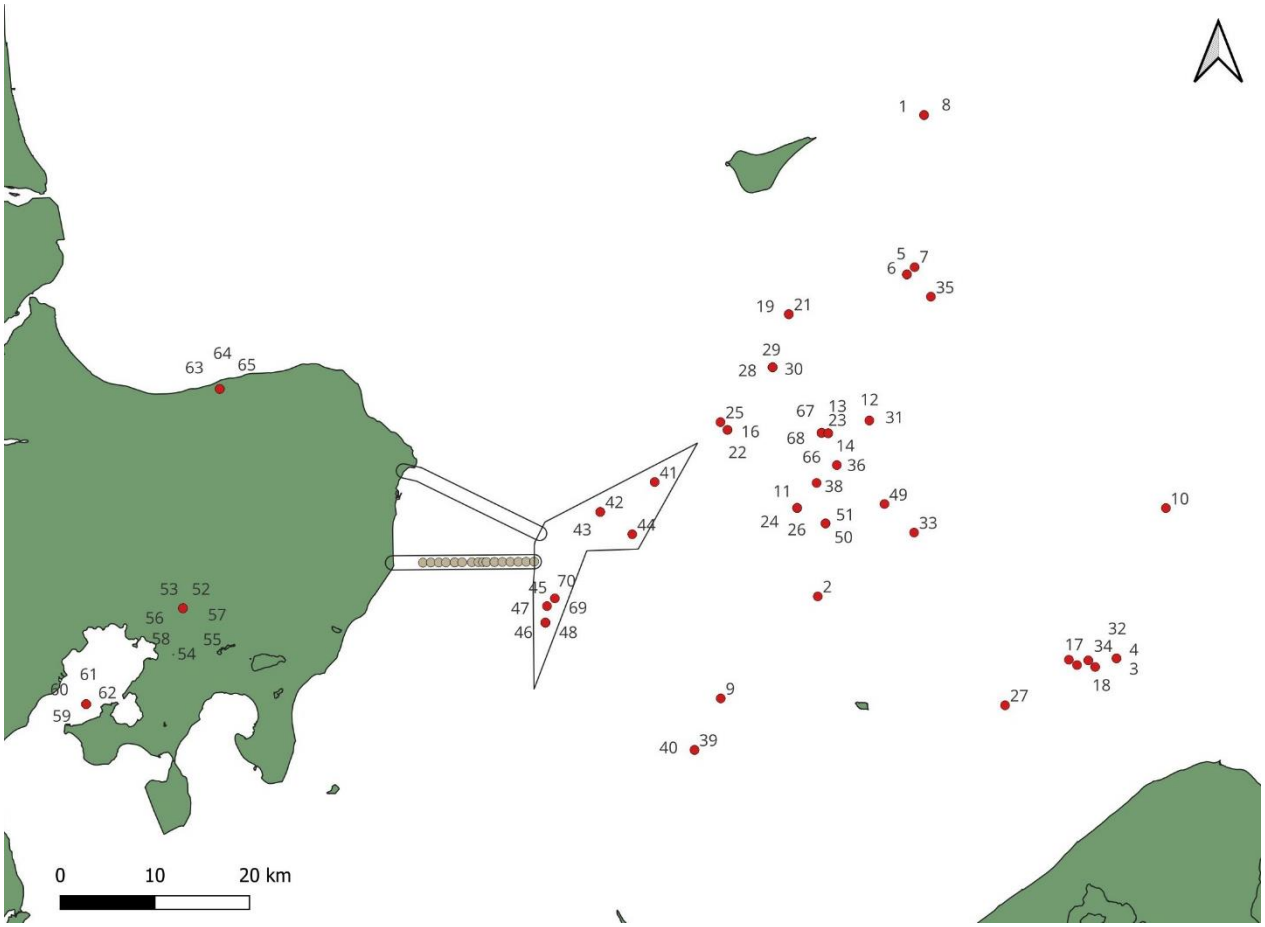

Figure 8 Distribution of sea-level index point that has been included in the Kattegat analysis (shown in red). Numbers refer to ID number that is shown in Appendix 6.3 and in sea-level curve in Figure 9.

To determine prehistoric sea-levels it is crucial to have access to well-dated material. We have compiled an overview of dated samples from the Kattegat area judged to be representative of the project area (See Appendix 6.3). These include samples which were either directly above or below the sea surface during the Late Palaeolithic and Mesolithic and they can thus be used to bracket sea levels and coastlines at various points in the past. At some depth and age intervals there are few points that can be used to determine sea levels. An agreement was therefore reached between Energinet and MAV to date samples from Kattegat to enable poorly covered intervals to be addressed with much greater precision.

All available core logs from the Kattegat project were reviewed to identify sediment samples from various depths suitable to produce a new shoreline displacement curve. MAV requested sediment samples from marine or terrestrial layers based on the core logs. Samples were sent to Moesgaard Museum where they were sieved with the goal of recovering material suited for dating. From the marine samples, primarily marine molluscs were chosen for dating, while from the peat layers it was either peat or wood (preferable small branches). All the shells were photographed before they were sent to the dating lab to subsequently determine whether the shells come from marine, brackish, or freshwater environments. It was ascertained that the dated specimens were exclusively marine molluscs, which suggests their findspot was below sea level at the time of deposition. On April 26th, 2024, MAV submitted eight samples to the Aarhus AMS centre from Kattegat and three samples Hesselø South. Moesgaard Museum received the results of these on the 20th of June 2024 (see Table 2 below).

Table 2 Radiocarbon dated samples from Kattegat and Hesselø South. Contextual information about the samples can be found in Appendix . 14C ages are reported in conventional radiocarbon years BP (before present = 1950) in accordance with international convention (M. Stuiver & H.A. Polach 1977). Thus, all calculated 14C ages have been corrected for fractionation so as to refer the result to be equivalent with the standard δ13C value of -25‰ (wood). δ13C values have been measured by AMS only and are not reported since the values obtained here are not as precise and therefore only indicative regarding association with the terrestrial/marine/freshwater food chains

AAR	Sample ID	Name	Material	Yield (%)	^{14}C yr. BP	Calibration Program		Calibration Options	Calibrated Age 95.4% (2σ)
38163	46762	HS_S_11_BH PO2 B1	shell	65,7	9101	42	OxCal v4.4.2 Bronk Ramsey (2020); r:5	Marine20 DeltaR: 52.0 ±25,0	7821BC (95.4%) 7460BC
38164	46763	HS_S_11_BH PO1A	wood	52,9	8861	50	OxCal v4.4.2 Bronk Ramsey (2020); r:5	IntCal20	8228BC (95.4%) 7791BC
38165	46764	HS_S_06_BH PO2 T1 B3	shell	71,5	9057	48	OxCal v4.4.2 Bronk Ramsey (2020); r:5	Marine20 DeltaR: 52.0 ±25,0	7764BC (95.4%) 7386BC
38166	46765	KG_25_BH PO2 B2 x5	shell	78,3	4545	42	OxCal v4.4.2 Bronk Ramsey (2020); r:5	Marine20 DeltaR: 52.0 ±25,0	2757BC (95.4%) 2327BC
38167	46766	KG_25_BH PO2 B2 x6	wood	42,6	9148	53	OxCal v4.4.2 Bronk Ramsey (2020); r:5	IntCal20	8542BC (6.5%) 8511BC 8486BC (88.9%) 8275BC
38168	46767	KG_07_BH PO1 B2 x7	shell	57,1	2129	30	OxCal v4.4.2 Bronk Ramsey (2020); r:5	Marine20 DeltaR: 52.0 ±25,0	320AD (95.4%) 635AD
38169	46768	KG_07_BH PO1 B1 x9	shell	71,1	4207	34	OxCal v4.4.2 Bronk Ramsey (2020); r:5	Marine20 DeltaR: 52.0 ±25,0	2278BC (95.4%) 1897BC
38170	46769	KG_12_BH PO3 B2 x4	shell	77,3	7538	44	OxCal v4.4.2 Bronk Ramsey (2020); r:5	Marine20 DeltaR: 52.0 ±25,0	5976BC (95.4%) 5656BC
38171	46770	KG_25_BH PO1 B2 x11	nutshell	59,9	8871	45	OxCal v4.4.2 Bronk Ramsey (2020); r:5	IntCal20	8231BC (82.6%) 7931BC 7923BC (12.8%) 7820BC
38172	46771	KG_25_BH PO1 B2 x10	shell	79,7	4815	32	OxCal v4.4.2 Bronk Ramsey (2020); r:5	Marine20 DeltaR: 52.0 ±25,0	3066BC (95.4%) 2681BC
38173	46772	KG_02_BH PO3 B2 X8	shell	76,7	4230	31	OxCal v4.4.2 Bronk Ramsey (2020); r:5	Marine20 DeltaR: 52.0 ±25,0	2305BC (95.4%) 1925BC

2.5.2. Modelling sea levels – creating a shoreline displacement curve

A sea-level curve shows relative sea levels at various points in time in relation to present day sea-level. The curve that was made for this project is based on existing dated samples (for example, those collected for the Hesselø South OWF and other projects. For samples to be included in the analysis they must meet the following criteria: 1) they provide information about prehistoric sea levels, 2) they have been recovered in a secure context, (in-situ), 3) they have vertical placement information, and 4) they are absolutely dated (e.g. with radiocarbon dating). Table 2 shows the result of the radiocarbon dates from the planned area of Hesselø South and Kattegat sent for dating. Additional contextual information about all the dated samples that are included can be found in Appendix 6.3. while Figure 8 show the spatial distribution of the radiocarbon dated samples that has been incorporated in the new sea-level curve.

The sea-level curve in Figure 9 is created by entering the uncalibrated C14 ages and vertical placement information (masl) into an MS Excel spreadsheet after which it was imported into the online calibration software OxCal. The ages were modelled in OxCal after age and vertical location using the depth model function. Samples are calibrated and shown in the shoreline displacement curve with a 95.4% confidence interval. Previous dates that were done at the radiocarbon lab in Copenhagen on marine samples have a built-in correction for the marine reservoir effect so no additional correction was done for this study. Marine samples dated at the AMS laboratory (in Aarhus and other laboratories) were corrected for a reservoir effect of 400 years. After this correction dates were finally calibrated suing the IntCal20 curve (Reimer et al. 2020) and plotted in a curve after the vertical location versus age.

The shoreline displacement curve shows marine samples in blue (for example, marine shells), terrestrial samples in green, and samples coming from sand or gyttja layers which may come from the coast or a lakeshore in grey. All the fixed points on the curve were assigned a number (R_Data) that can be referenced in Appendix 6.3 (column “id”) so it is possible to see additional information about the individual samples that are dated.

The dashed line in the new sea-level curve gives the hypothesized sea level in the planned cable route area in the Holocene. Furthermore, Table 3 summarizes sea-levels at different times as they appear on the curve. It can be seen from the curve that there is a relatively good correlation between the marine- and terrestrial samples with the latter typically situated above the marine. It is not possible, however, to determine sea levels precisely at depths ranging from – 10 to – 20m due to a lack of sea-level index points within this interval. On top of that is the uncertainty associated with dating shells and peat, combined with the still long intervals where there are few dates to use for determining sea levels. Another issue that affects the shape of the curve is the isostatic rebound that has changed the vertical position of the samples used in the shoreline displacement reconstructions. In general, lands to the NE of the OWF area and cable routes have been lifted more than those to the SW. Thus, it is problematic to include points from a wide geographic area in the same curve. Because the degree of difference in rebound within the area is not known precisely, it is not corrected for in this curve.

The new sea-level curve shows that the relative sea-level reached its lowest level around 11,000 BC (13,000 BP) 30 m meter lower than now. This was followed by a rise in sea-levels from ca. 10,000 BC (12,000 BP) continuing throughout the Holocene. Jensen and Bennike (2020) presented another sea level curve from this area (Figure 10). It suggests a fall in sea-level until c. 11,000 BC (13,000 BP) when it reached a level approx. 30-35 m below that of today. This corresponds to the lowest recorded terrestrial sea level index point (SLIP) used in Figure 9. If the sea-level curves are representative there

should be little to no archaeological Stone Age potential in the areas of the OWF that lies deeper than 30-40m. Both curves also suggest a sea-level rise from at least 11,000 BC (13,000 BP). However, a notable lack of terrestrial SLIPS within the area makes it very difficult to determine the prehistoric sea-level with sufficient details.

This indicates that all land surfaces in the OWF area was transgressed during the Maglemose culture (11,500-8,400 BP) and that human presence during the Kongemose (8,400-7,400 BP) and Ertebølle (7,400-6,000 BP) is restricted to the cable route.

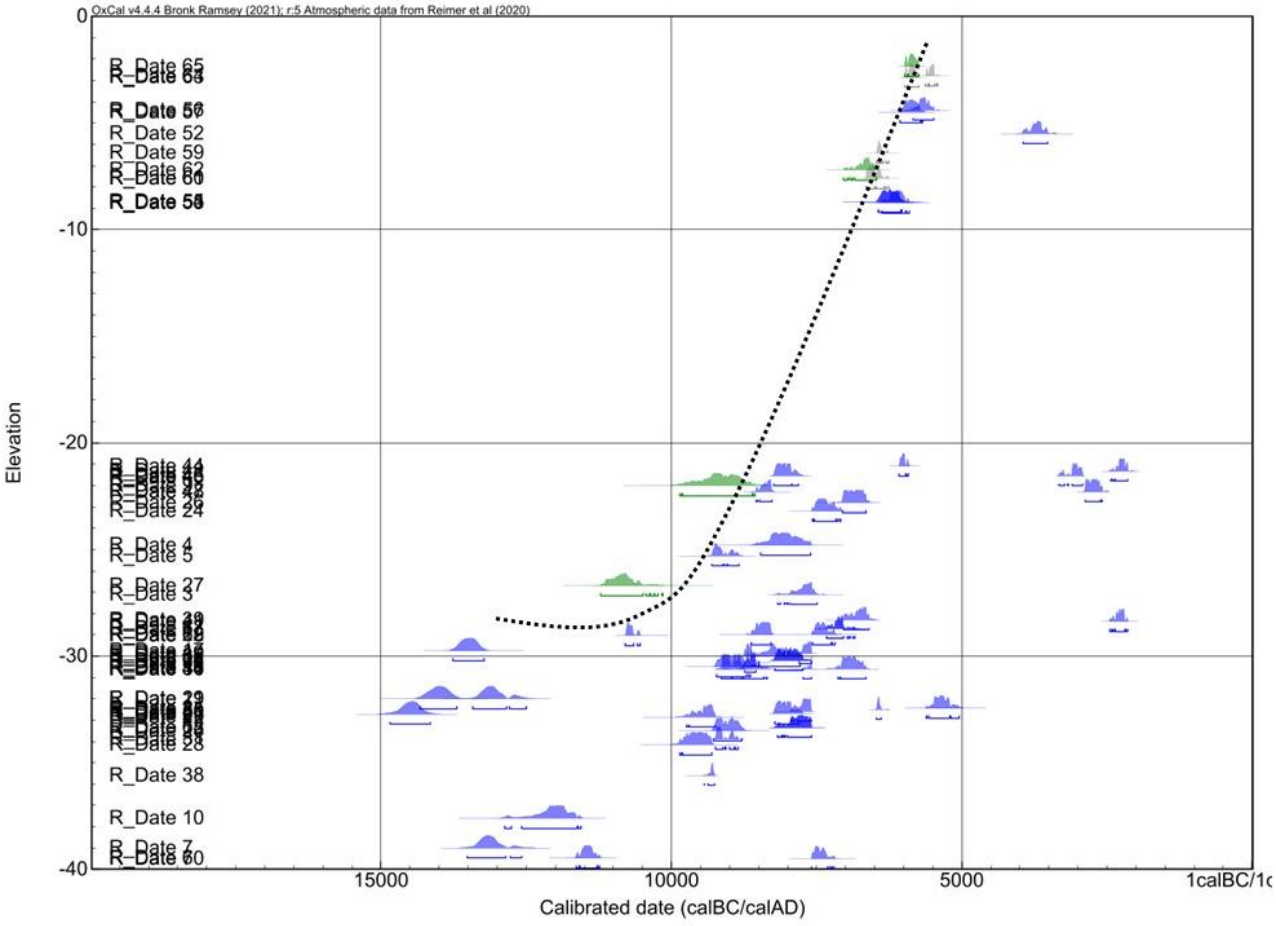

Figure 9 Shoreline displacement curve where the dashed line gives the hypothesized sea level in the planned area since the late glacial maximum. Marine samples are shown in blue whereas terrestrial samples are shown in green. Grey samples refer to samples from archaeological sites that represent accurate sea-level index points.

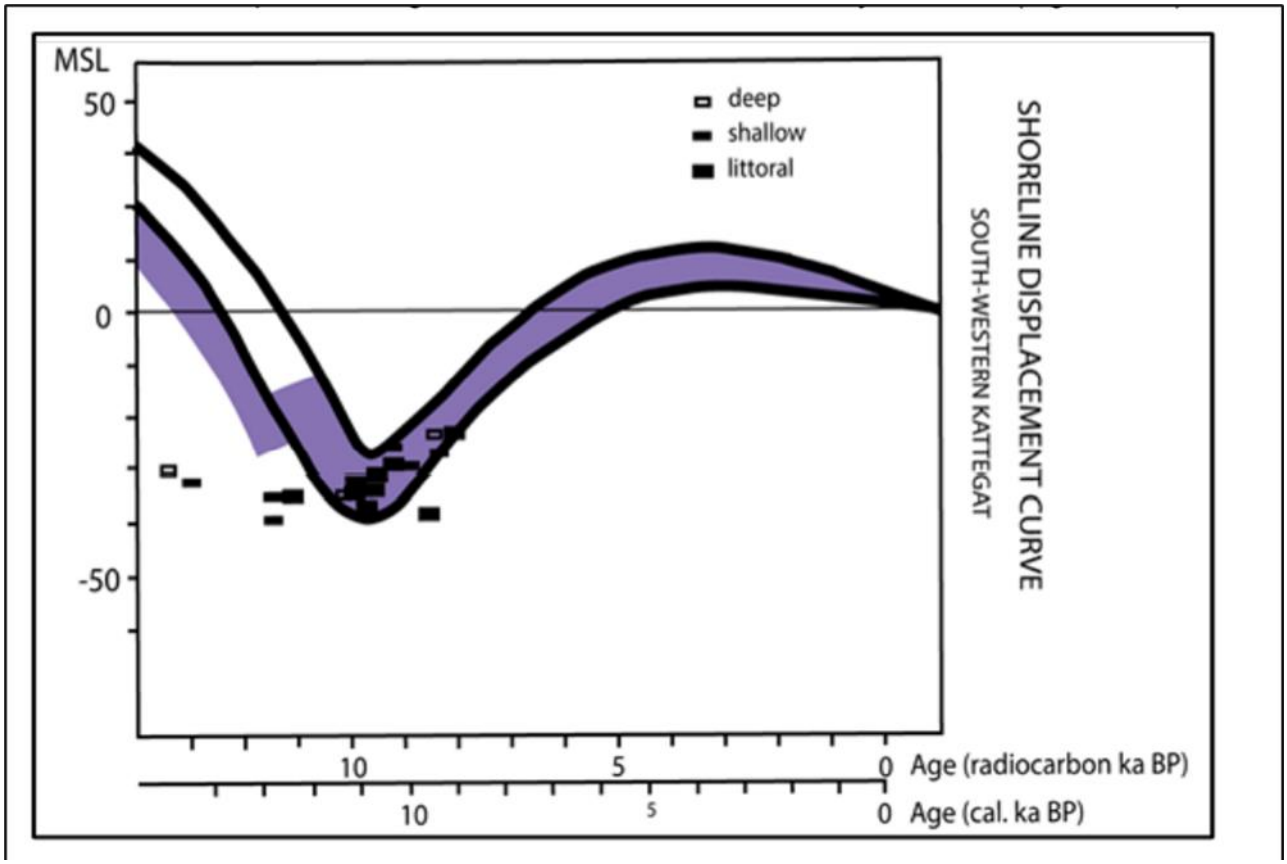

Figure 10 Shoreline displacement curves for the southern Kattegat. The two solid black lines indicate the range of shoreline displacement in non-faulted regions of the study area. The purple area indicates the relative sea level changes interprets from the sequence stratigraphy in the downfaulted NW-SE striking depression. Radiocarbon dated samples are indicated as deep > 10m, Shallow 2-20m or littoral 0-2m. After Jensen and Bennike (2020).

Table 3 Sea-levels as they appear on the sea-level curve in Figure 9.

Time	**Sea-level**
11000 BC / 13.000 BP	-28 m
10000 BC / 12.000 BP	-27 m
9000 BC / 11.000 BP	-23 m
8000 BC / 10.000 BP	-17 m
7000 BC / 9.000 BP	-10 m
6000 BC / 8.000 BP	-4 m

2.5.3. Sub-bottom seismology and landscape correction

The Geophysical and Geological survey report provided by GEOxyz presents an overview of the interpreted seismic surfaces/horizons (see Table 4). Four horizons are identified to represent boundaries between different sediment layers in the subsurface, with each layer corresponding to a specific depositional environment. Together with available geological literature from the area, the depositional environment, seismic facies and soil type of the units were interpreted allowing us to describe the geological development in the Kattegat area.

Understanding the seismic units and horizons is essential for coastal geology, as varying sediment types impact erosion and sedimentation, influencing historical coastline positions. The horizon grids (tiffs) are used to model former coastline positions, because they provide a more accurate picture of the prehistoric landscape compared to the modern seabed bathymetry.

Table 4 Seismic horizons, units, along with their soil types and depositional environments, are presented. Figure sourced from the Geophysical and Geological Survey Report for Kattegat by GEOxyz.

Unit	Upper surface	Lower surface	Main Soil Description	Depositional Environment
I, H, Holocene	Seabed	H05	Silty, sandy CLAY with thin veneer of SAND at seabed	Post-glacial marine
II, GL, Late Glacial	Seabed/H05	H20	Variable, includes intervals of laminated CLAY, SAND-prone packages	Periglacial, glaciomarine
III, GL, Glacial	H05	H30	Variable, CLAY-prone, locally overconsolidated	Glacial with localised direct ice contact
IV, BR, Bedrock	H20/H30	-	Various carbonates and clastics. Possible crystalline basement	

2.5.4. Interpreted horizons and units in the Kattegat OWF site

This section presents the interpreted geological horizons and units presented in the Geophysical and geological survey report by GEOxyz. The surface geology of the Kattegat area is marked by a broad, meandering channel feature, ranging from 750 to 1650 meters in width, which runs northeast to southwest across the northern and central sections of the site. In the northern section, this channel is well-defined and deep, but it becomes shallower and less distinct toward the south. The area is bordered by boulder fields, and trawl marks of various orientations are present particularly in the central and northern regions.

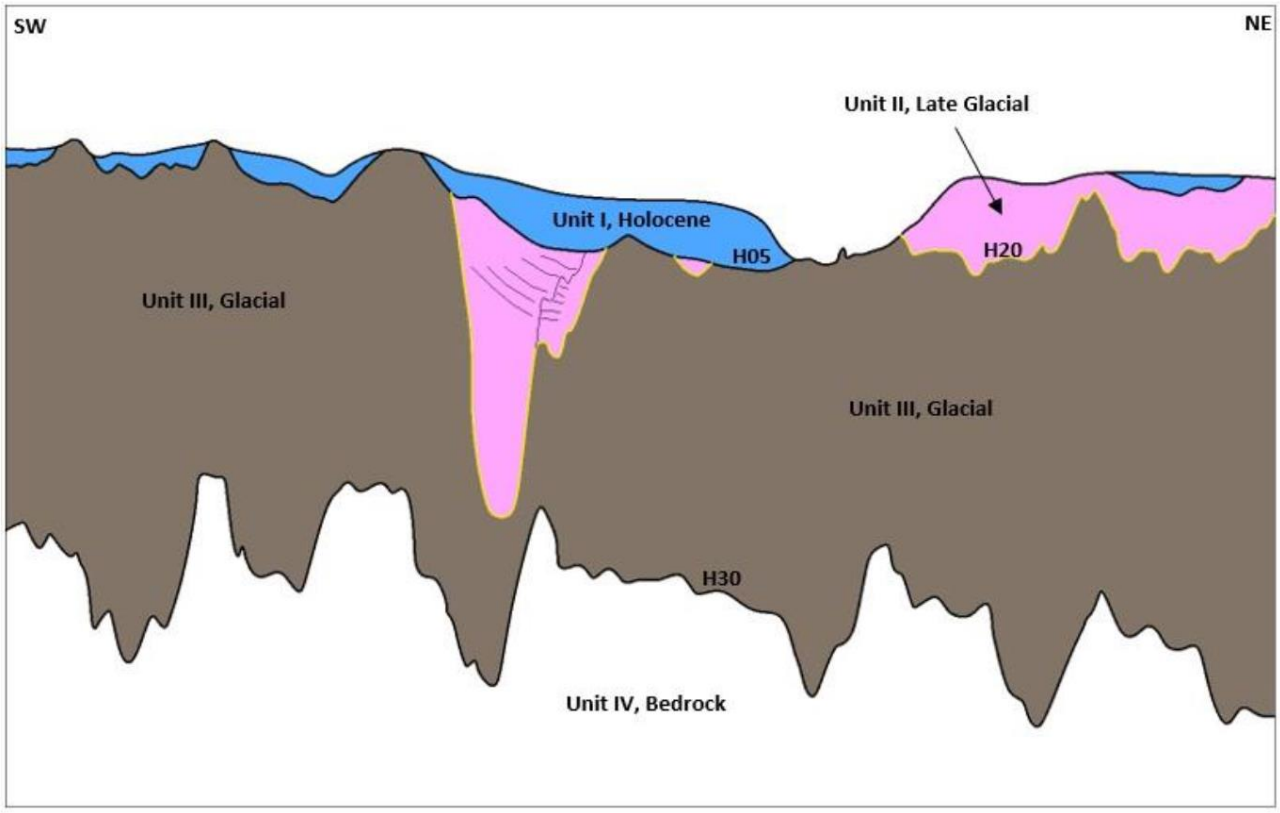

Figure 11 Seismostratigraphic interpretation, displaying the mapped horizons and the interpreted seismic units from the Geophysical and Geological survey report from GEOxyz (2023).

2.5.4.1. Unit IV – Bedrock

The Geological report by GEUS (2020) showed that the bedrock in the Kattegat OWF area consists of Jurassic sandy mudstone to Lower Cretaceous limestone. The Grenå-Helsingborg Fault runs NW/SE through the Kattegat OWF area.

2.5.4.2. Unit III – Glacial

The report by GEOxyz describes unit III as a glacial deposit linked to the LGM around 22,000 years ago. The base of this unit is marked by horizon H30. The unit consists of till with a typical thickness between 24 m to 40 m, however it locally reaches a thickness between 2 m to 90 m. This unit is subdivided into two units (H and G) in the Geological report by GEUS (2020). The unit comprises overconsolidated clay-rich diamicton with silt, sand, gravel, cobbles, and boulders (Geophysical and Geological survey report from GEOxyz, 2023).

2.5.4.3. Unit II – Late Glacial

Unit II is complex due to the environmental changes that occurred during the Late glacial to Holocene. It is marked by horizon H20 at its base. This unit both consists of intervals of laminated silt and clay, and sandy beach type deposits (Geophysical and Geological survey report from GEOxyz, 2023). Due to the complexity of the unit, the Geological report by GEUS (2020) also subdivided the Late Glacial unit into three units (D, E, and F) that marks basin infill of glaciomarine, glaciolacustrine or glaciofluvial sediments.

2.5.4.4. Unit I – Holocene

The Geological and geophysical report by GEOxyz described Unit I as the Holocene unit. The Holocene deposits in the study area consist of a marine post glacial silty, sandy clay layer. These sediments are thinly distributed (<1.5 m) and often absent in the northern and southern sections, where glacial till lies close to the seabed. The maximum thickness of the unit is around 9.5 m, and observed within a SW to NE trending channel with a width of around 1 km. Here unit I comprises infill of the channel.

In the Geological report by GEUS (2020), the Holocene unit has been subdivided into three units (unit A, unit B and unit C). Unit C consist of marine medium-grained sand, and is interpreted as a near coast deposit, such as spit bars or barrier islands, and formed during the Early Holocene (Geological report by GEUS, 2020). Unit B was described as early Holocene interlaminated to interbedded clay with silt and shells. The depositional environment for this unit was interpreted as a deltaic environment at the mouth of the Dana River system (see Figure 4). Unit A overlies Unit B, and consists of marine clay to clayey, medium grained sand or sand gytja (Geological report by GEUS, 2020). Unit A is interpreted as a marine Holocene sediment.

For the Kattegat area a decision was made to apply horizon H5 that marks the transition from Late glacial to base of the Holocene unit. The horizon was provided in GeoTIFF format to the geoarchaeological analysis. The coastlines in H5 were drawn using the raster calculator in QGIS by selecting cell values within the compiled H5 model that were below the sea level of the time. The sea level used for the different models were chosen based on Table 3, where estimated sea-levels from the sea-level curve are shown. The areas below sea level (in different points in time) were subsequently transformed from raster areas to polygons. Areas where the horizon is absent are marked in grey on the coastline models.

2.6. Coastline models

It appears from the coastline models (Figure 12-Figure 17) that the former landscape in the OWF area underwent a massive transformation from 11,000 to 6,000 BP. The oldest model (Figure 12) depicts a freshwater river/paleochannel that drained the Ancylus lake into the Kattegat through the Dana River (paleo-Great Belt channel). From the younger coastline models it is difficult to determine exactly when the marine/brackish water entered into the river system and when the channel changed from a freshwater environment to a narrow fjord system. The water that is depicted in scenario 11,000 and 10,000 BP (Figure 12-Figure 13) is believed to be the outlet from the Anculus / Dana River. However, during the Littorina transgression marine water gradually entered the freshwater outlet. On the basis of the sea-level curve and geological studies (e.g. Bendixen 2017) it is assumed that the area was fully marine no later than 9,000 years BP.

The 9,000 BP model is the only one that can be used to map the position of the coastlines in the area. Only 1000 years later the whole OWF area had been transgressed by the Sea. Any potential Stone Age material / sites in the areas must therefore have to date from the Upper Palaeolithic cultures and/or the early Mesolithic Maglemose culture. It is possible that the area closest to land was habitable during the Kongemose- and Ertebølle cultures, but the poor data coverage in the model of H5 prevents the coastlines in those areas to be reconstructed.

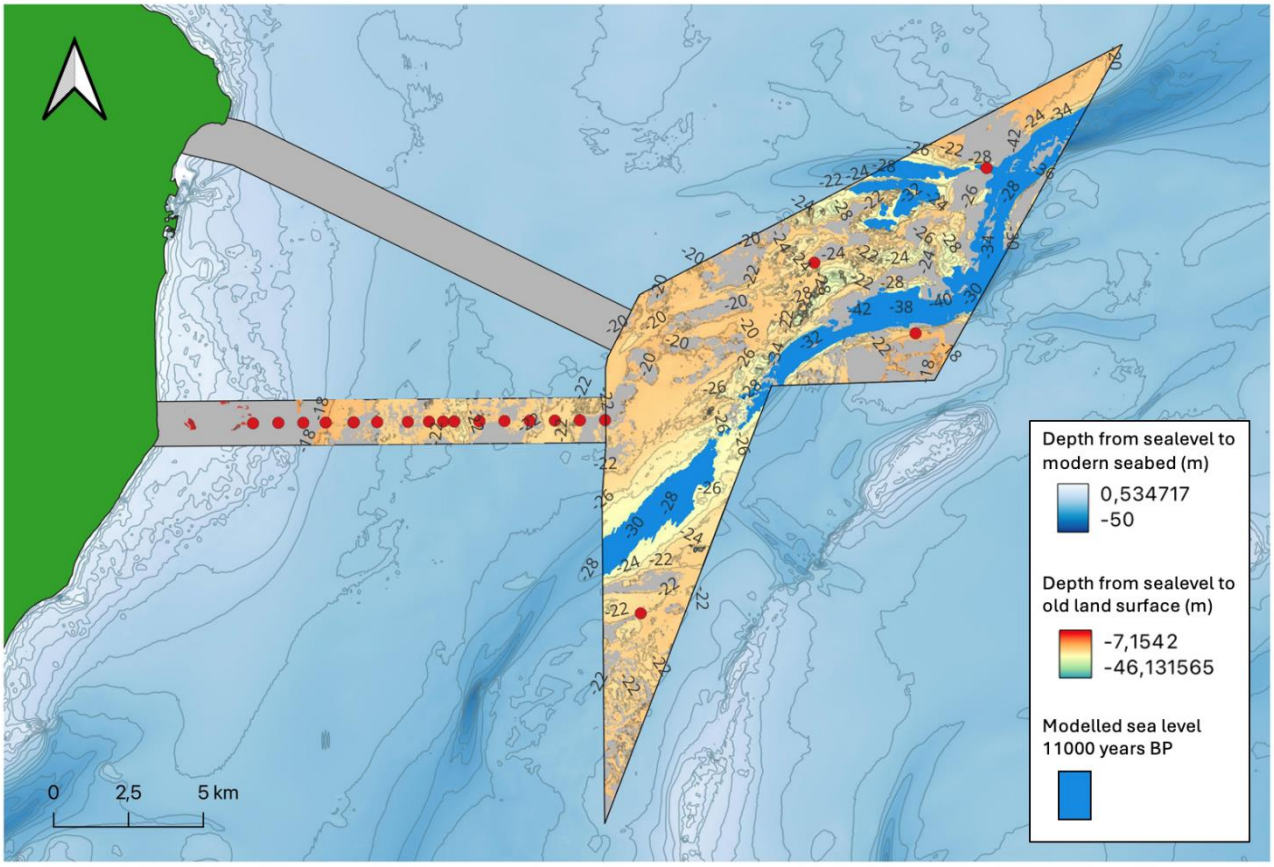

Figure 12 Modelled palaeochannel / river at ~11.000 years BP, showing inundation of lowest topographical areas. Contour lines outside the OWF site and cable routes represent modern bathymetry below sea level. Red dots indicate the borehole locations.

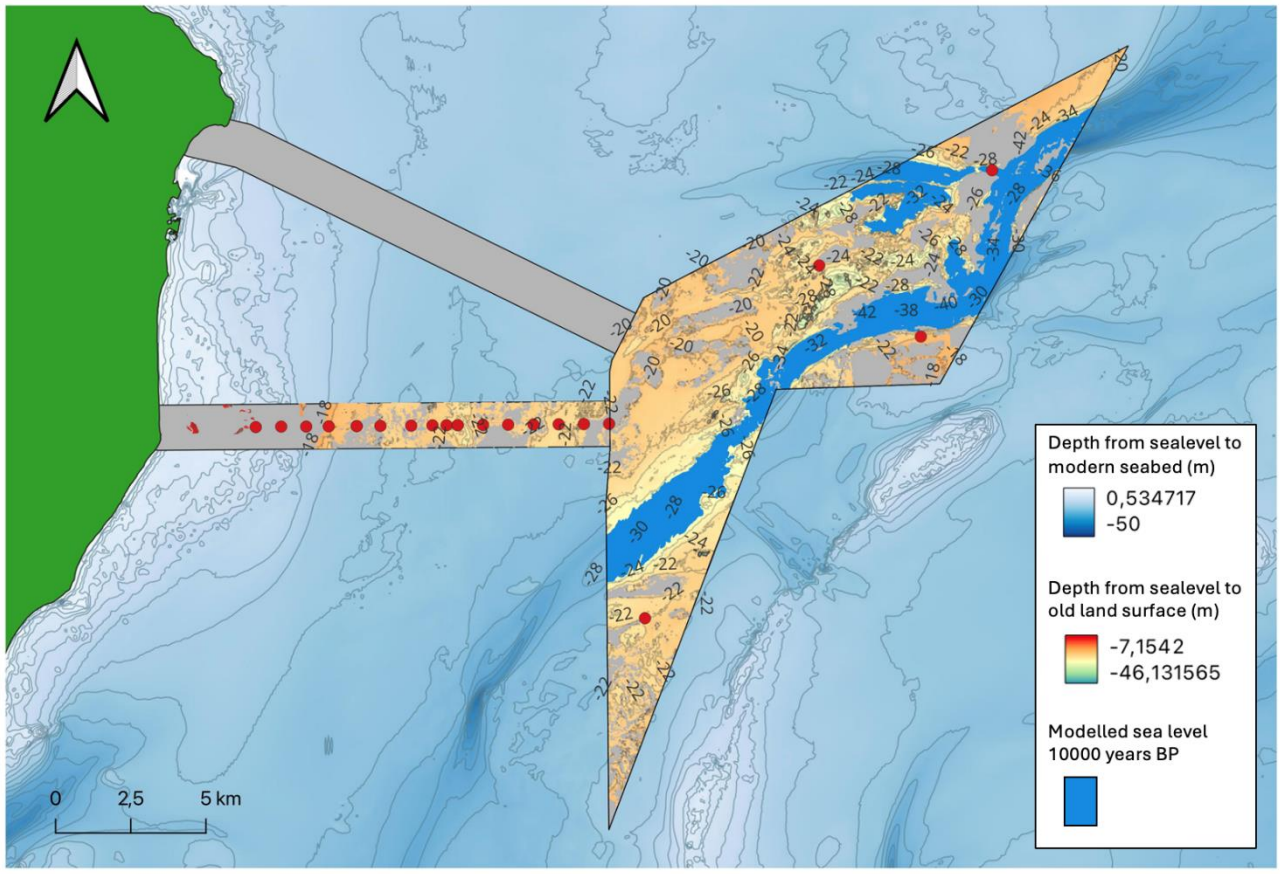

Figure 13 Modelled river or coastline at ~10.000 years BP, showing inundation of lowest topographical areas. Contour lines outside the OWF site and cable routes represent modern bathymetry below sea level. Red dots indicate the borehole locations.

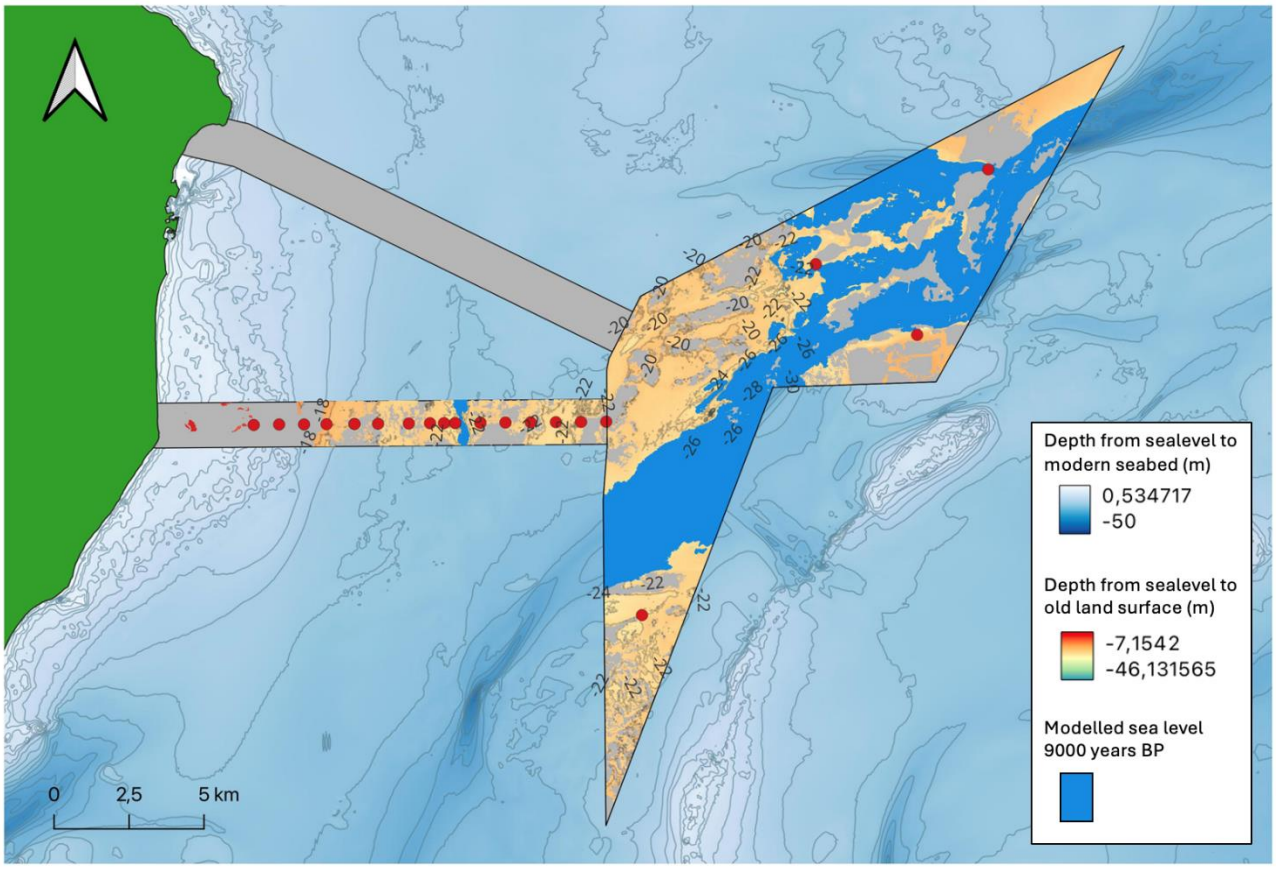

Figure 14 Modelled coastline at ~9.000 years BP, showing inundation of lowest topographical areas and around these. Contour lines outside the OWF site and cable routes represent modern bathymetry below sea level. Red dots indicate the borehole locations.

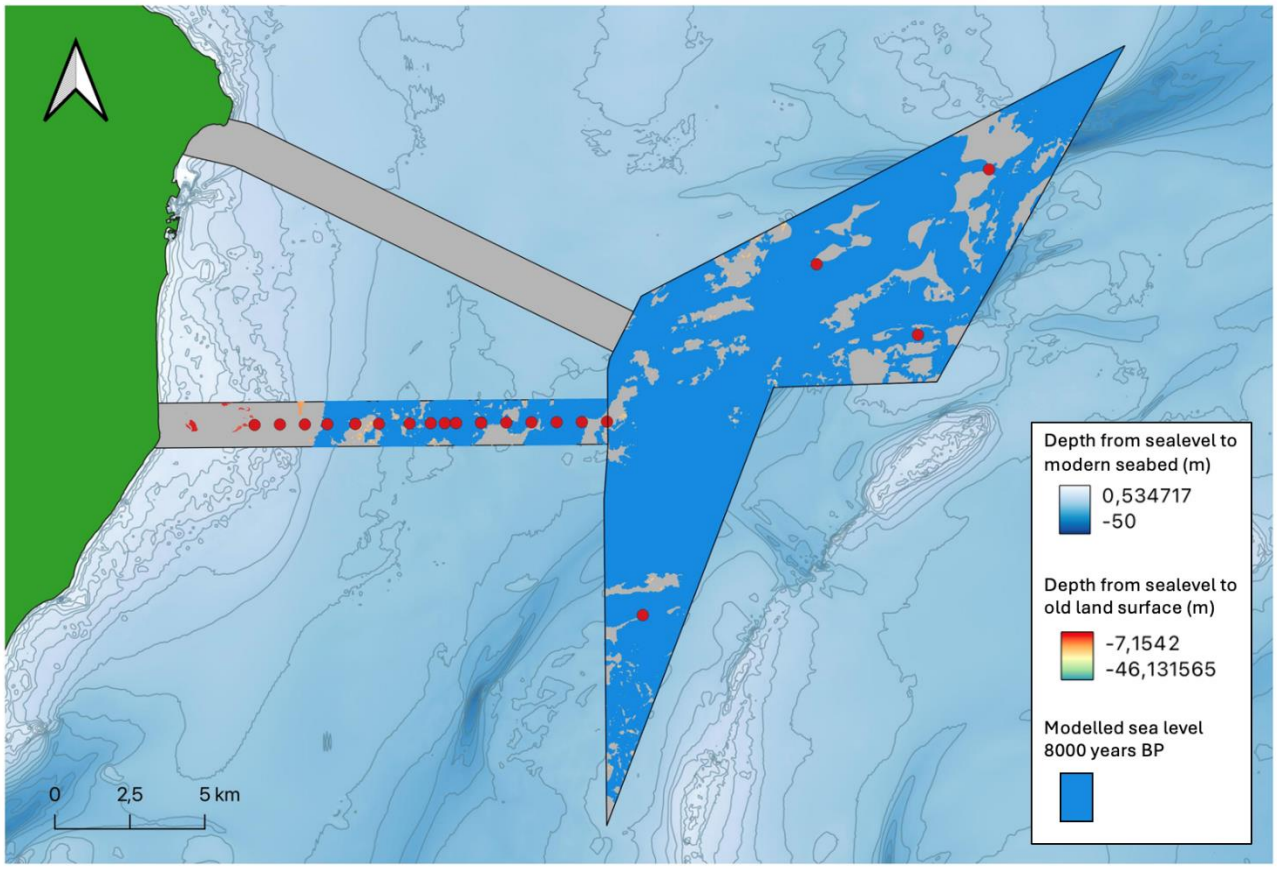

Figure 15 Modelled coastline at ~8.000 years BP, showing inundation across the site and cable routes. Only a smaller area near the Danish coastline has not been flooded. Contour lines outside the OWF site and cable routes represent modern bathymetry below sea level. Red dots indicate the borehole locations.

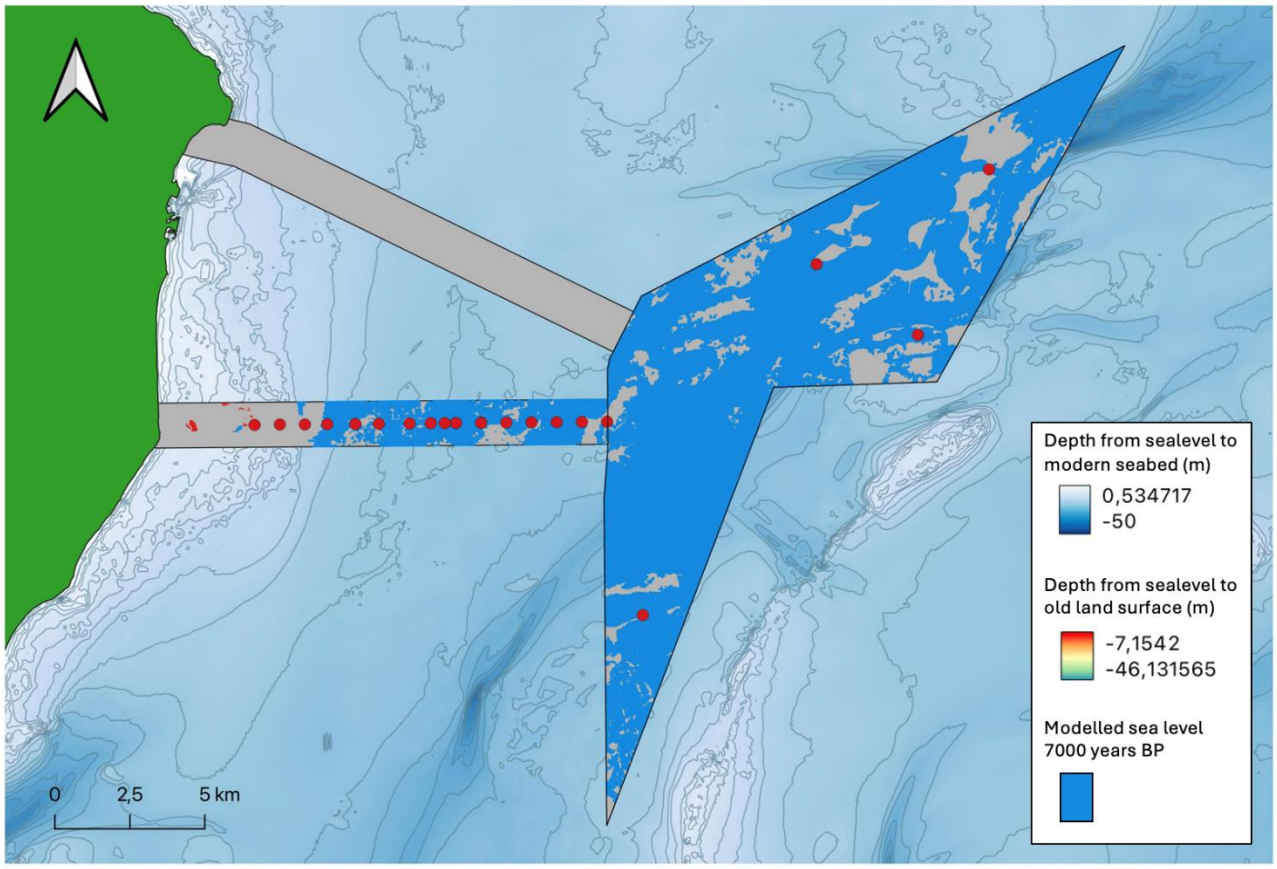

Figure 16 Modelled coastline at ~7.000 years BP, showing inundation across the site and cable routes. Only a smaller area near the Danish coastline has not been flooded. Contour lines outside the OWF site and cable routes represent modern bathymetry below sea level. Red dots indicate the borehole locations.

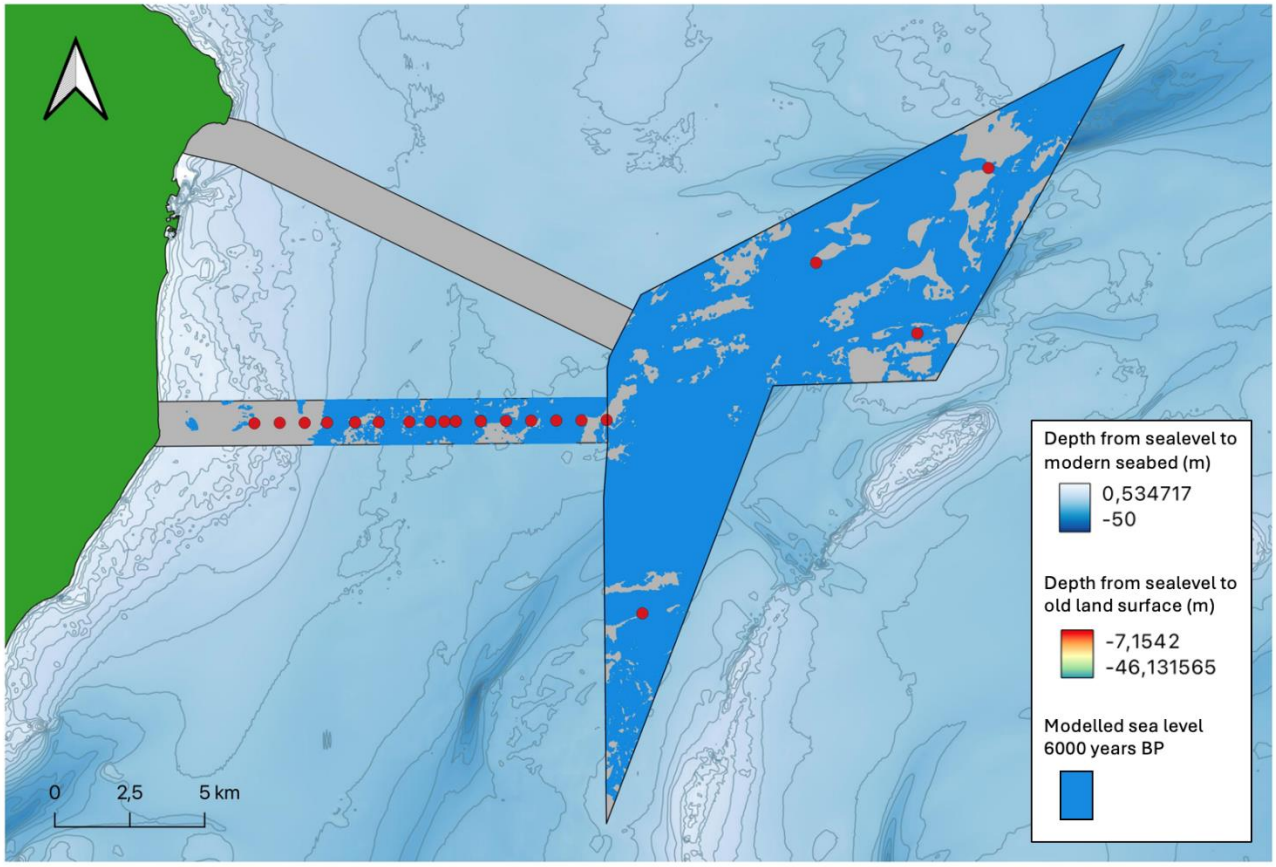

Figure 17 Modelled coastline at ~6.000 years BP, showing inundation of the whole site and cable routes. Contour lines outside the OWF site and cable routes represent modern bathymetry below sea level. Red dots indicate the borehole locations.

2.7. Areas of archaeological interest

2.7.1. Former coastlines and river outlet areas

Normally in a geoarchaeological analysis, the reconstructed landscape is used with topographic models (e.g., the fishing site model for coastal areas) to designate areas where it is believed there is an increased likelihood of human activities. However, any archaeological sites in the OWF area will have to predate c. 8,500 BP and so little is known about the extent to which people lived along the coasts in the area. Research projects from other parts of Denmark suggests that the former coastlines are likely to have been places where people preferred to position their sites (Astrup 2018). For this reason, we will attribute greater archaeological potential to coastal areas suitable for fishing (e.g. areas near fjords, streams, etc.) compared to former inland areas that were not in the immediate vicinity of lakes and streams. In addition, we ascribe greater value to the areas where the rivers flowed into the sea. The reason being that river deltas are considered to have been particularly rich in resources. It is also in such areas that many of the sites from the Kongemose- and Ertebølle cultures have been found. It should be said, however, that the coastlines were only habitable for a short period of time before the coast moved again. This had a direct impact on the amount of archaeological material that could be deposited in a given coastal area within the Kattegat area. Coastal sites may consequently be hard to detect in some areas because it was not possible to have as many repeated sites/habitations in areas that witnessed rapid sea-level rise compared to a stable coastline.

2.7.2. Former lake and river environments

Traces of the early Mesolithic societies in southern Scandinavia have so far primarily been located along former lakes and rivers systems that later changed to bogs. There are equally good reasons to believe that people also favored wetland resources in the Kattegat area. The big channel most likely functioned as a river in the early Mesolithic and therefore it is likely to be a good place to search for sites (given that it is in such environments most of the pre-boreal sites in Denmark have been recorded). We believe that the areas surrounding the streams and lakes have greater archaeological potential than other inland areas. Areas along the rivers and lakes were also habitable longer than the coastal areas where sea-level rise made areas uninhabitable. It can be difficult to find settlements that were positioned close to freshwater basins (lakes and streams) since these are often at risk of being buried under thick layers of younger sediments. Fortunately, Energinet has provided grids and core logs that show the minimum distance from the modern seabed to layers with Stone Age potential. The isopach grids show where it is difficult to reach layers with archaeological Stone Age potential and where it is unlikely that cables etc. will cause any damage to Stone Age sites. The selections of areas for archaeological surveys are planned in areas that were suited for settlement where past sedimentation allows such investigations without extreme difficulty in accessing the layers. Energinet´s isopach models was used to identify and prioritize areas with a thin sediment cover (less than 2m) on top of horizon H5.

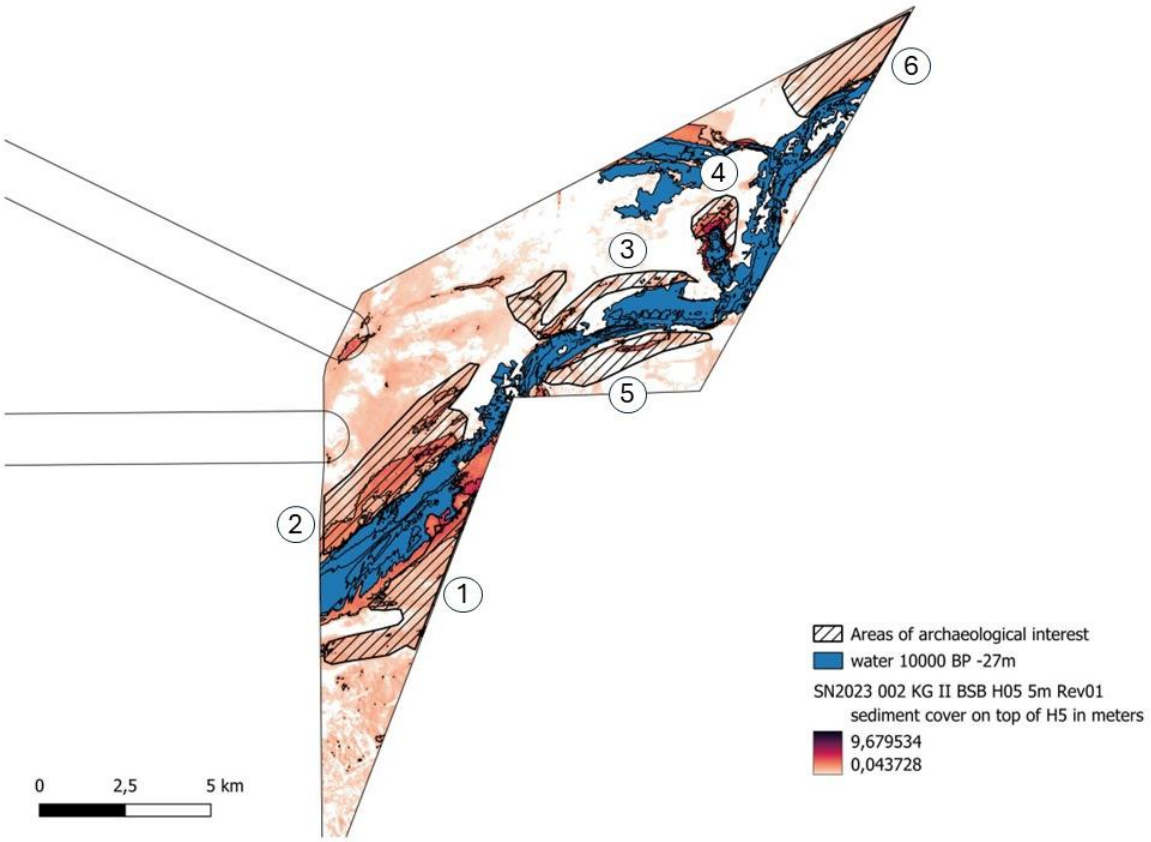

Figure 18 Areas of archaeological interest. Shown according to sediment cover on top of H5 and a sea-level that corresponds to the time around 10.000 BP.

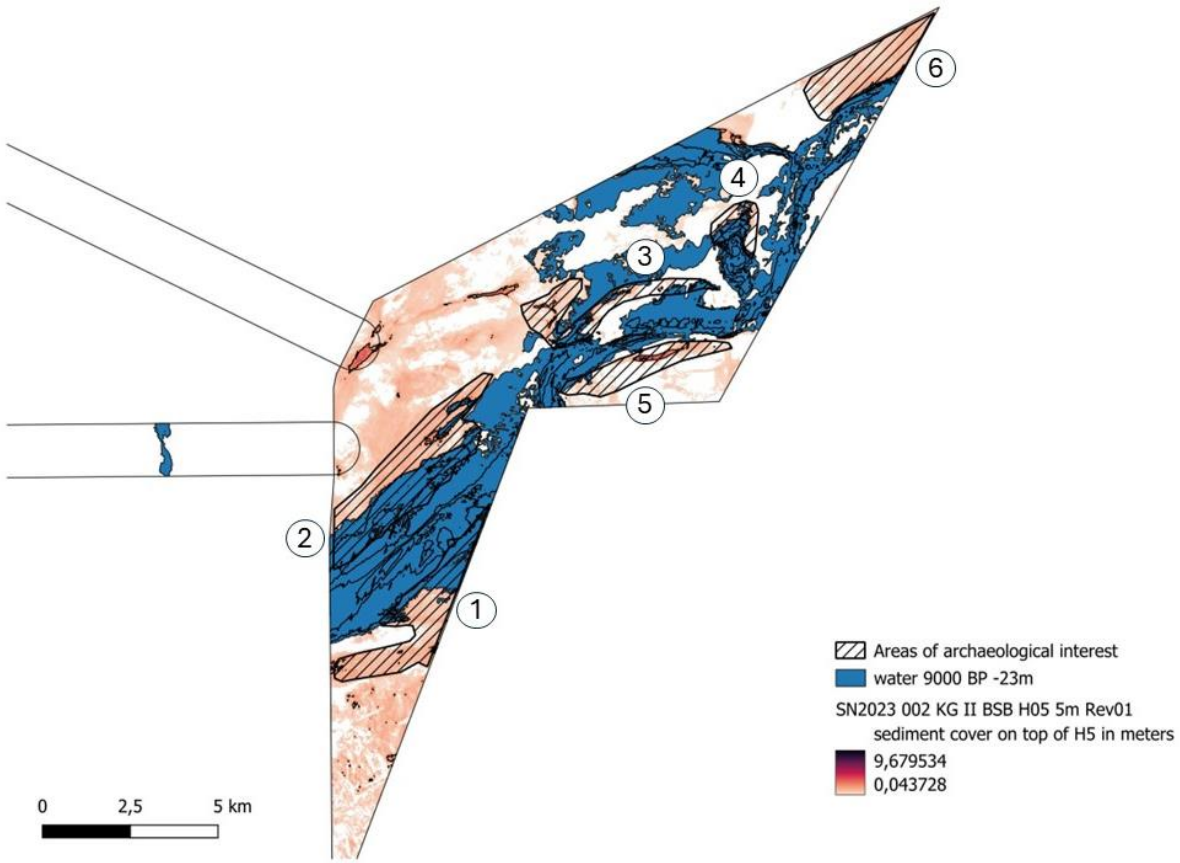

Figure 19 Areas of archaeological interest. Shown according to sediment cover on top of H5 and a sea-level that corresponds to the time around 9.000 BP.

2.8. Recommendations regarding submerged Stone Age archaeology

The scale of the Kattegat project allows us to present a relative coherent picture of a landscape that once consisted of forests, rivers, lakes, fjords and hunter-gatherers. Our rationale for the selection of the various areas with the highest potential can be summarized as follows:

All areas were located close to the river where people had access to fish and freshwater resources. It would also have been possible to inhabit the same areas at a later time when the sea came into the area. Thus, it is possible to find settlements in the same areas that were originally placed to utilize different types of resources. (i.e. everything from the reindeer hunters in the late Paleolithic to early Mesolithic groups that utilized the resources in the river system and potential subsequent coastal cultures). That it was possible to utilize the same areas, for different purposes, at different times, can be said to create a greater probability that some of the archaeological assessments which form the basis for the designations are correct.

The areas are selected because of topographical features (e.g. the fishing ground model) and because potential archaeological material is considered to be accessible in these areas because the sediment cover on top of H5 is less than 2m.

2.9. Conclusions regarding submerged Stone Age archaeology potential

MAV has reviewed the data provided by Energinet and completed a desk-based geoarchaeological analysis of the geophysical survey. The geoarchaeological analysis concludes that construction works pose a threat to prehistoric sites in the Kattegat OWF area.

The Kattegat project covers an enormous area of approximately 147 km^2. Six areas have been selected because of their topographical characteristics and features (e.g. the fishing site model) and because potential archaeological material is considered to be reachable in these areas because of a limited sediment cover. It is suggested that an agreement is made between the developer, SLKS and MAV as to how (and how many) positions that should be examined in a subsequent archaeological test excavation survey. We cannot exclude the possibility of Stone Age material in the cable routes but do not believe there is sufficient justification for attempting to detect them.

3. Submerged historical archaeology

Geophysical data provided by Energinet was used for this geoarchaeological analysis. The comprehensive specifications for the data collection, equipment, technical details, data processing and interpretation methods can be found in the report Geophysical and Geological Survey Report for Kattegat by GEOxyz and provided by Energinet.

3.1. SSS- and MBES anomaly selection

As part of the geoarchaeological analysis, SSS- and MBES-data were analysed with the software SonarWiz ver.7 and ver.8, and then subsequently exported to QGIS and MS Excel for further analysis. Here, the data was screened systematically by a team of archaeologists at MAV with experience in geophysical data analysis. In this process, targets already found by the geophysics team were reviewed. The work was organized by survey blocks, as outlined in the Geophysical and Geological Survey Report for Kattegat by GEOxyz.

Relatively recent wrecks can often be spotted in SSS data. But wrecks, which have lain exposed to the sea over a longer period, cannot easily be identified. Wrecks will be so degraded that they are difficult to identify or, even if well-preserved, they may be covered by bottom sediments. The migration of sediments, especially close to shore in the ECR area, will conceal and then occasionally uncover wrecks and remains temporarily.

There were distinct differences in some areas regarding the density and number of contacts marked in the SSS-data, as well as the line spacing and number of MAG-anomalies. Especially two corridors in the ECR-area showed many fewer contacts that the rest. In the OWF-area, survey block B01 had a much larger density of contacts than the other blocks.

In the ECR, the change in the density of anomalies correlates with the change in seabed surface sediment and the correlation is similar, though not as clear-cut, in the OWF area. There is an increase in the number of MMO-contacts over till/diamicton compared to muddy sand/mud or sand.

SSS-data was primarily used for analysis to identify potential cultural historical objects and cross-checked with other data sources. Anomalies selected in other datasets were marked in the MMO-list, even if not visible in the SSS-dataset.

Anomalies were chosen based on whether their character indicated potentially man-made objects that were lost over 100 years ago and therefore protected by the Danish Museum Act.

The anomalies designated as “Boulder” by GeoXYZ were not ignored when they correlated with MAG or MBES anomalies or otherwise with points of interest.

3.2. Wreck databases

The SSS data will thus only show the situation at the time of survey. Other important sources are the existing databases of wrecks. For the historical cultural heritage analysis, the following databases were reviewed among others:

- Danish central register of cultural historical properties, Fund og Fortidsminder, Slots- og Kulturstyrelsen, https://www.kulturarv.dk/ffreg/
- Danish sports divers´ wreck database, Vragguiden, https://www.vragguiden.dk
- Danish Maritime Authority´s register of wrecks (Søfartsstyrelsens vragdatabase).
- Royal Navy Loss List database, MAST Maritime Archaeology Sea Trust, https://www.thisismast.org/research/royal-navy-loss-list-search.html
- Data over lost Allied aircraft from 1939-45 (https://www.airmen.dk/)

Insofar that the wrecks registered here are not visible in the SSS data, they can be covered by sediment at the time of surveying but are still present in the seabed.

It must be made clear that the positions recorded in these databases often are inaccurate. Some of the data stem from the Danish Maritime Authorities, where for instance a ship would for instance have been reported to have sunk certain miles in a cardinal direction from a point. While a geographical point can be set at that exact position, it is obviously not a precise location for this wreck.

In other cases, ships have only been recorded to have vanished in a broad water area. Such 'administrative' positions act as a placeholder to mark that wrecks are somewhere in the general area.

An important source behind the registered wrecks are fishermen reporting snagged fishing gear, or authorities reporting sunk vessels. The positions reported are not always very precise, and they stem from a long period of time, using very different navigational techniques, from dead reckoning to GNSS.

In terms of geographical precision, the databases of wrecks are the weakest data. Oppositely these data are strong in terms of evidence, as they often build on archival material, in which case the identification and dating of the wreck is certain. Some wrecks in the databases have later been salvaged.

For further review of the archival data see Dalicsek 2023.

3.3. MAG-targets

The SSS anomalies were also cross-checked with the MAG targets provided by Energinet. As older wrecks in the area will most likely be covered by sediment, the original MAG data (raster format) were also reviewed. Minor anomalies can be explained by debris being lost or dumped from vessels, and thus are less important here. Larger anomalies, in nT values or in spatial extension, are highly likely to represent wrecks.

MAG-anomalies with a P2P-value of 40nT or greater were automatically selected for further inspection, although the anomaly list includes those associated with known modern shipwrecks. An internationally accepted standard in maritime archaeology to identify wrecks from magnetometry data is a P2P value of 50 nT. In this case we have set a more restrictive threshold or either +20 nT or -20 nT. Nominally this gives a P2P threshold of 40nT, but in practice both peaks are not always seen clearly in the data. This depends on the distance and orientation of the target to the survey line. As such a more restrictive approach makes sense in this context to target all signals of importance. 40nT would indicate wreck debris sizeable enough for archaeological identification (for further methodology on MAG surveying see Michael 2011 and James 2024).

Due to the use of a single sensor setup, the sampling rate is high along the survey lines but is distanced widely between the lines. As such MAG data cannot pinpoint the location of a wreck (cf. the Best Practice document). But with the use of protection zones around the centre of the strongest signals, it is possible to prevent hidden wrecks from being damaged during construction. It is obviously not possible to assess with certainty whether these signals represent wrecks, nor if they are older than 100 years.

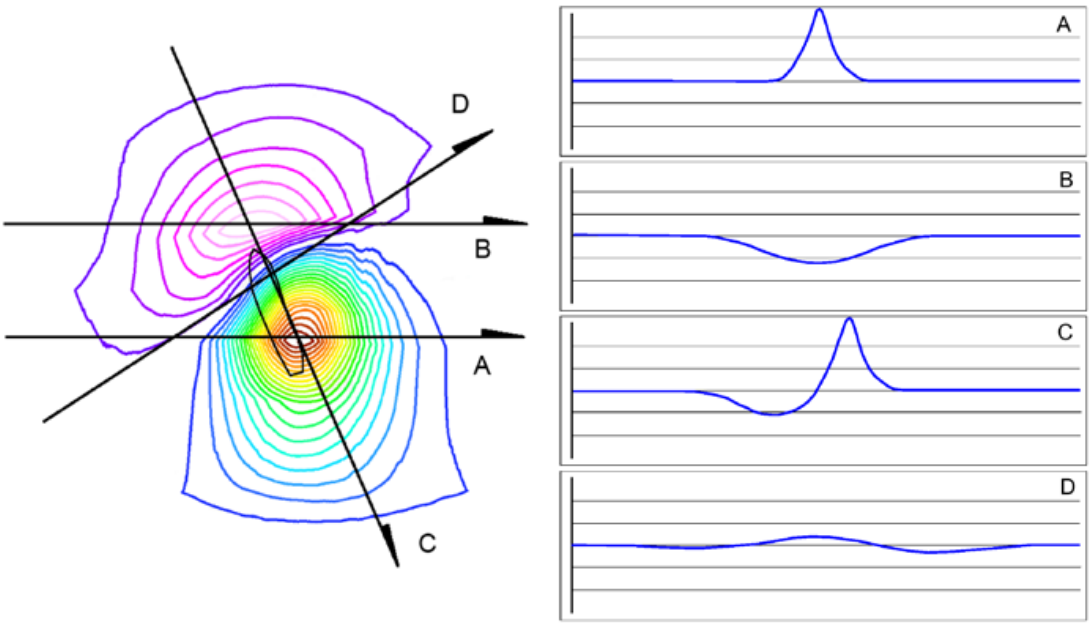

Figure 20 Armed trawler HMT Elk (L×B: 31.1 × 6.4 m, mined 1940). The magnetic field model, and examples of the resulting magnetic response at various curses through the magnetic field. After Holt 2019: Fig. 8.

Illustrating the potential MAG responses to a target relative to the survey transect, Holt (2019). It can be seen how a transect right along the wreck (track C) will produce the classical + - anomaly in the data, while other courses may give only positive or only negative responses. Indeed, a transect right at the border between positive and negative anomaly will hardly any response at all.

In the Kattegat dataset the known wreck of M/S TOPSY, a steel hulled ship of 150GRT and 30m LOA, has a MAG anomaly of 187,7nT at a distance of 32m from the centre of the wreck and no anomaly at all at a distance of ca. 50m. With a survey line spacing of 62,5m a complete wreck of the same size could go unnoticed if it lay between the lines and oriented along the main lines.

3.4. Confidence and significance

The MMO-anomalies, in addition to the classifications used by GeoXYZ, were divided into five categories to indicate their importance and likelihood as cultural historical objects.

CONFIDENCE 1 are those that are most likely archaeological objects.

CONFIDENCE 2 are those that are more uncertain and include the most interesting anomalies for a maritime archaeological survey.

CONFIDENCE 3 are those anomalies where the character and age of the object cannot be determined, but it is classified as a man-made object (MMO). Therefore, it is just as likely that it is modern debris as it is an archaeological artefact. There is a chance that some of these objects are geological features/boulders. Linear features, such as ropes, SSS-contacts associated with buried MAG-anomalies often fall into this category. MAG anomalies without other indications (MBES/SSS/archival data) point to an object in the seabed. The object can potentitally be geology, modern MMO (incl pUXO), CHO (incl. pUXO). Therefore, these MAG anomalies are included in the category CONF 3.

CONFIDENCE 4 are those anomalies where the object is most likely not of archaeological interest. This can often be debris associated with fishing, such as parts of trawl equipment. Linear objects with a large MAG-anomaly suspected of being wires or soft ropes with metal threads are often included in this category. Anchor chains would fall into the CONFIDENCE 3 category. Trawl marks were also taken as indication for the age of anomalies. Where trawl marks, seen as modern, ran underneath an anomaly, the anomaly was interpreted as modern and put into CONFIDENCE 4. Even where GEOxyz classified an anomaly as MMO, it was given CONFIDENCE 4, if deemed to be of geological character by MAV.

Geological anomalies were not marked for the geoarchaeological study. Anomalies deemed as certainly modern debris or installation were marked as CONFIDENCE 5 for the geoarchaeological study.

All anomalies selected based on SSS, MAG or MBES were combined in the MMO list.

GEOxyz has selected 982 man-made objects (MMOs) in the OWF area. 17 points were added to this list from the MAG anomalies, so that 999 locations were analysed by MAV.

GEOxyz has selected 1439 MMOs in the ECR area. 13 points were added to this list by MAV from the MAG anomalies, so that 1452 locations were analysed by MAV.

CONF 1 and CONF 2 targets are listed in Appendices 16.1 and 16.2 and all targets are supplied in MS EXCEL files MAV2023-048_ECR_archaeology_targets_table.xlsx and MAV2023-048_OWF_archaeology_targets_table.xlsx.

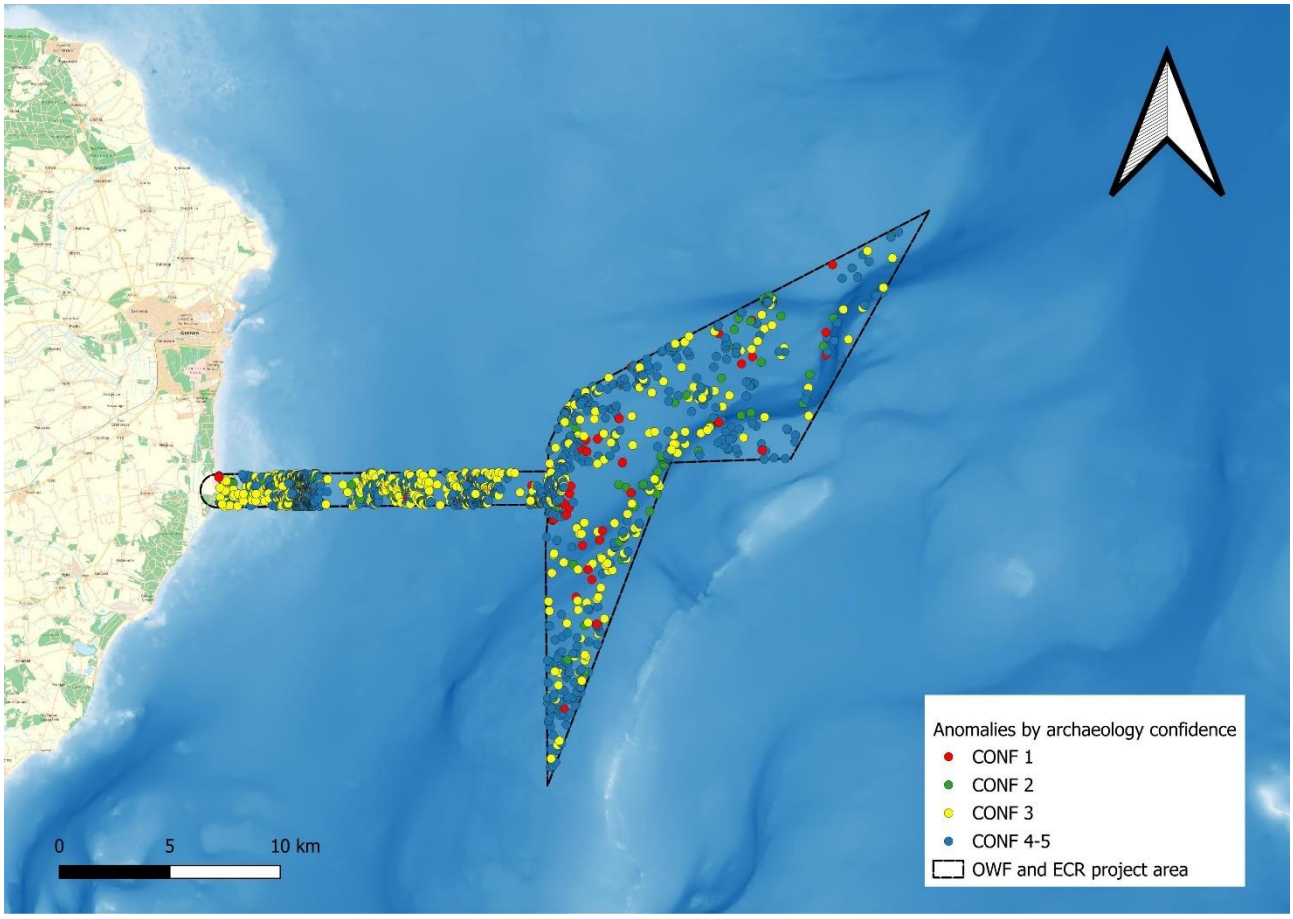

Figure 21All anomalies selected by archaeological confidence in the ECR and OWF project areas

3.5. SSS-anomalies

3.5.1. SSS-anomalies in the OWF-area

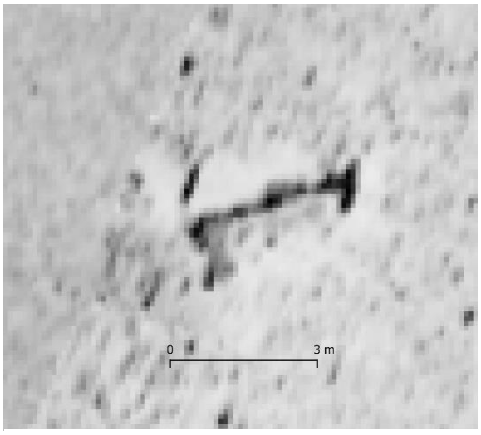

Figure 22 MMO Target ID413, an anchor in the OWF area, CONF 1 for archaeology

59 locations are defined by MAV as CONF 1. The anomalies include three anchors (Target ID 413,520,613). Three targets are grouped in the same location (within 2m of each other) and were defined by GEOxyz as "Boulder" (Target ID 985,986,987). These three targets are deemed MMO by Mav and due to their correlation with the registered location Vragguiden 2526 (76m W), are classed as CONF 1 for investigation. This should however not be taken as proof that the targets are (part of) a submarine wreckage. The target appears to be part of an anchor chain.

66 anomalies are defined by MAV as CONF 2, debris and anomalies where the anomaly's shape and/or surrounding seabed features could be of archaeological interest.

Figure 23 The wreck of M/S TOPSY in the SSS mosaic

221 anomalies are selected as CONF 3, these include debris of low or no magnetism, buried single or grouped contacts with no specific indicators for neither archaeology nor modern character and contacts with no other feature, but within 0,1NM of a known location from the consulted registers. This is the most difficult category to define whether it's an object or objects of archaeological interest or even an MMO.

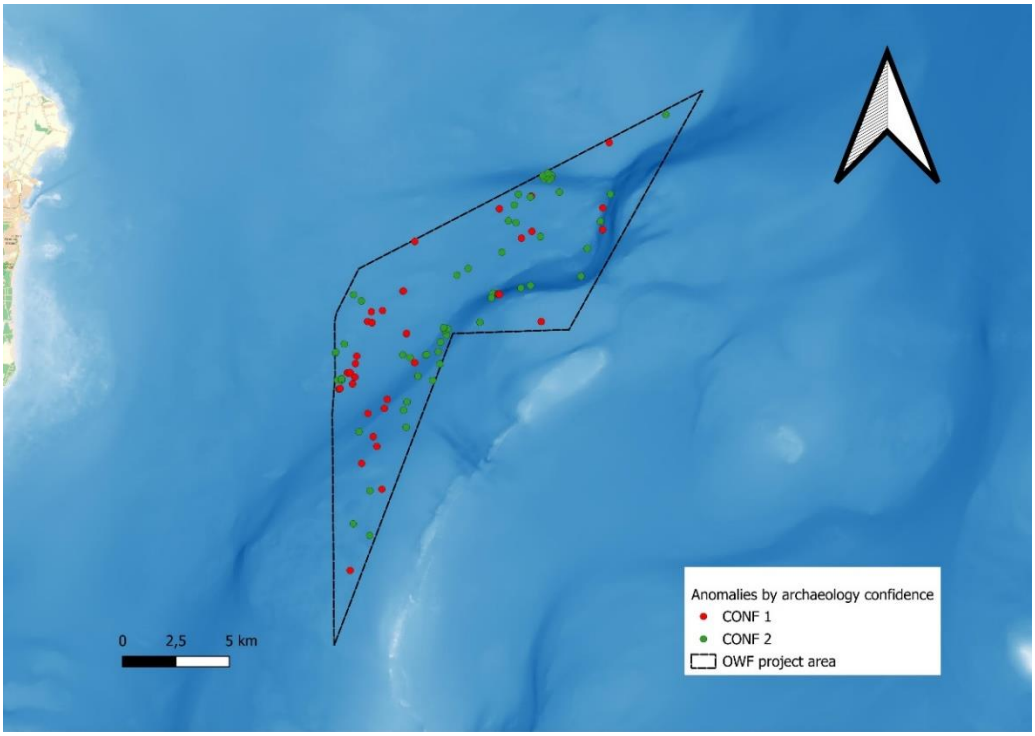

652 anomalies, classified by GEOxyz as MMO, were classified as CONF 4 and likely modern debris or geological anomalies.

The wreck of M/S TOPSY has been classified as CONF 5, a certainly modern object of no archaeological interest.

Figure 24 CONF 1 and 2 anomalies in the OWF project area

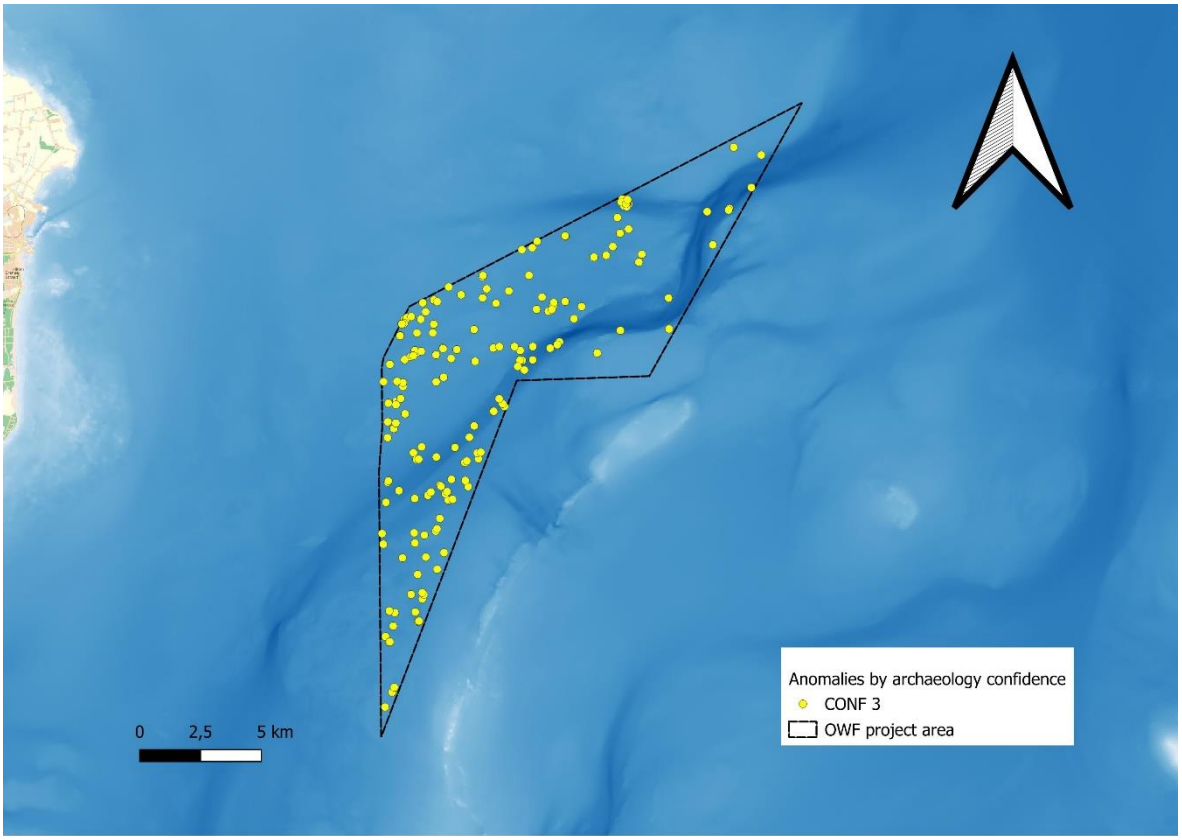

Figure 27 CONF 3 anomalies in the OWF project area

Figure 26 CONF 4 and 5 anomalies in the OWF project area

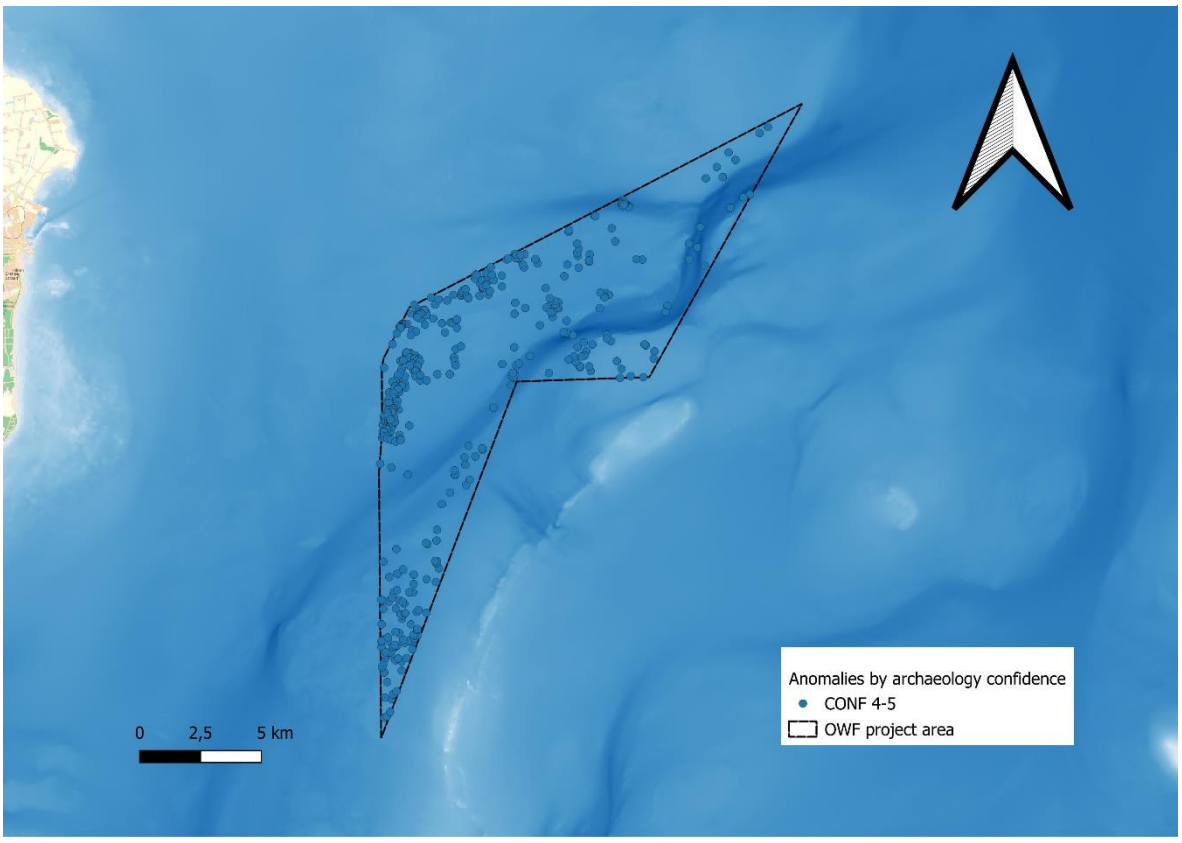

3.5.2. SSS-anomalies in the ECR-area

18 targets are defined as CONF 1 by MAV, five anchors (KG_ECR2_MMO_PTS_0702, KG_ECR2_MMO_PTS_0968, KG_ECR2_MMO_PTS_1153, KG_ECR2_MMO_PTS_1304, KG_ECR2_MMO_PTS_1138) and associated anomalies (9 targets alltogether) and two locations (KG_ECR2_MMO_PTS_1440, KG_ECR2_MMO_PTS_1443) (comprising 5 points) that cover strong MAG anomalies as well as SSS-contacts (selected by MAV, but not by GEOxyz), that also correlate with a previously registered archaeological find location. These two latter locations are within 165m from Systemnr 115536 in the Danish Central Register Fund- og Fortidsminder (FFM). The registered location is based upon the report of a fisherman from 1932, thus imprecise. Two soapstone (steatite) vessels were picked up at the location by the fisherman, and he reported more remaining at the location. The magnetic and associated SSS anomalies could be a shipwreck or wreckage with Viking age material.

47 anomalies are selected as CONF 2, these include various SSS anomalies deemed of archaeological interest.

561 anomalies were classified as CONF 3 and include debris with little or no characteristics to interpret. Several anomalies were included here that are within 0,1NM of a registered location. Some anomalies are associated with linear anomalies and can be modern fishing gear. Some MAG anomalies of 40nT P2P-value or greater were included here, as the source of the anomaly is likely buried.

The group of anomalies of CONF 4 include possible geological features and debris that is likely modern (i.e. fishing gear), or low value MAG-targets that are buried. 819 anomalies were classified as CONF 4.

7 anomalies are classified as CONF 5 and with most certainty not archaeological features, but likely geological.

Figure 28 Soapstone vessel from the Viking Age found on the Jutland coast Photo: Østjyllands Museum

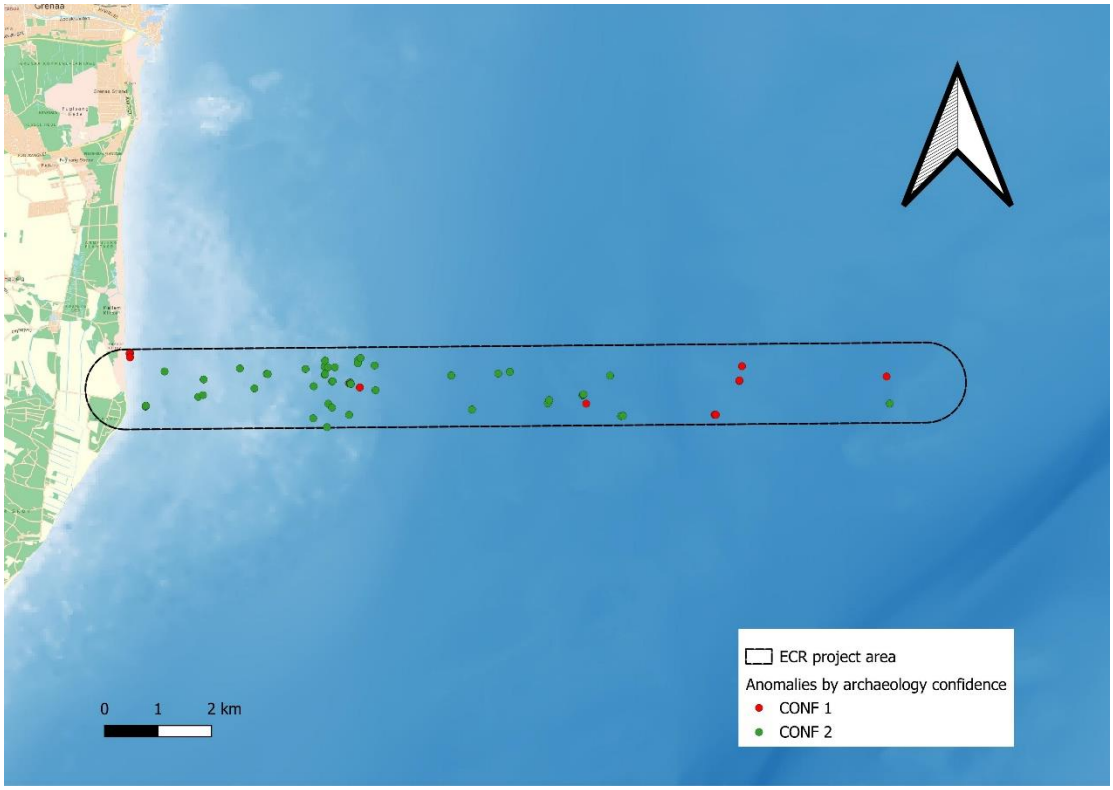

Figure 29 CONF 1 and 2 anomalies in the ECR project area

Figure 30 CONF 3 anomalies in the ECR project area

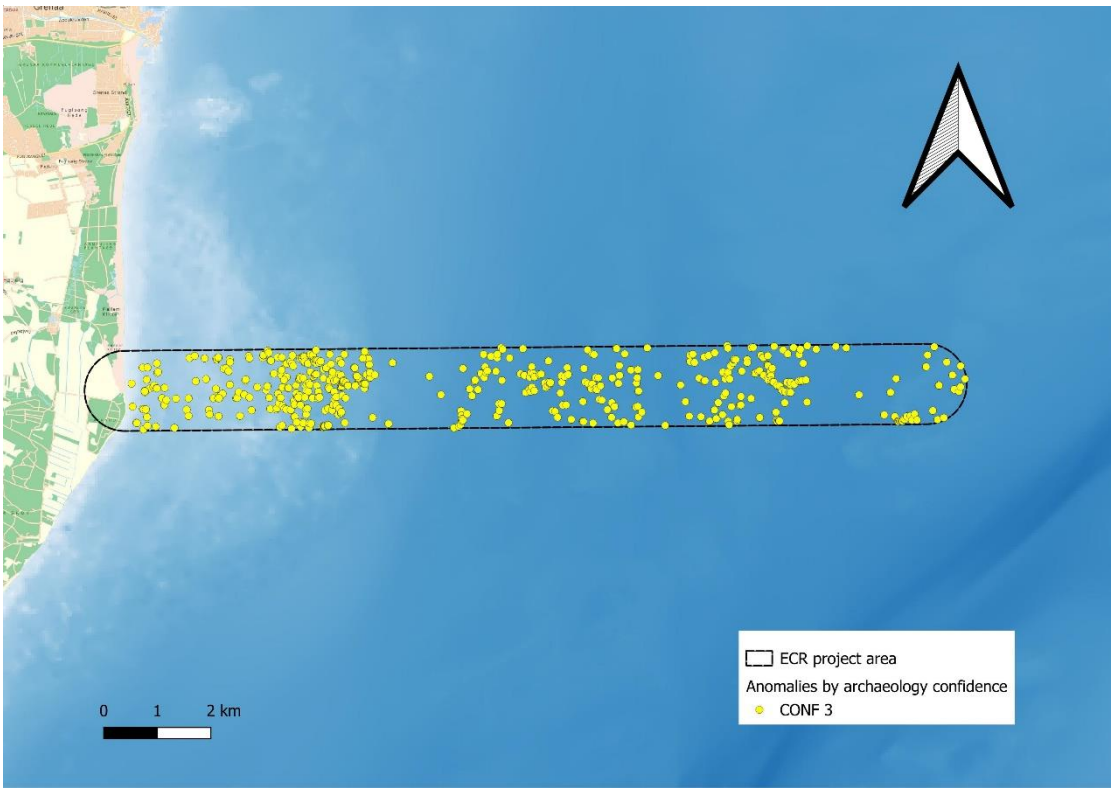

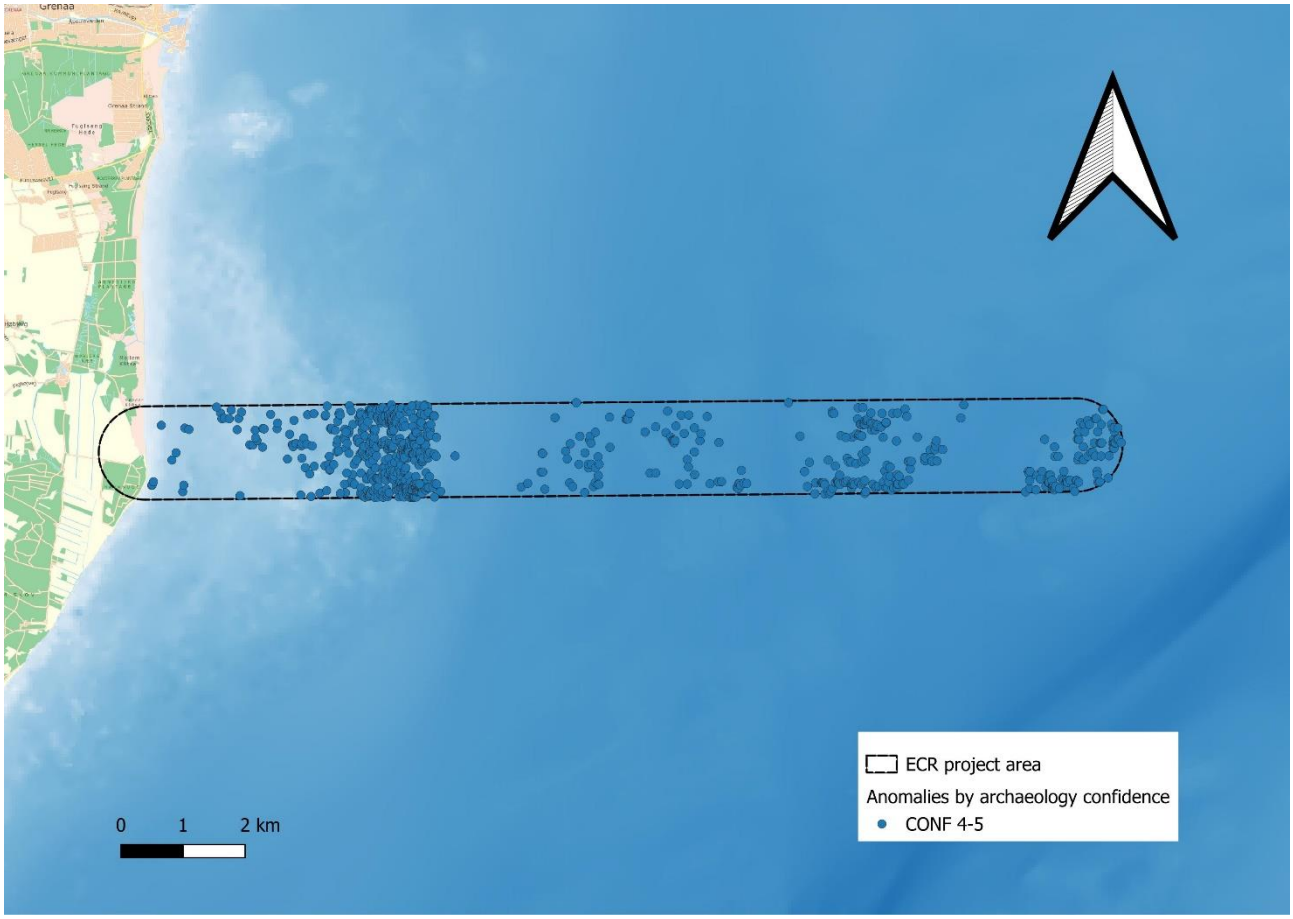

Figure 31 CONF 4 and 5 anomalies in the ECR project area

3.6. MAG-anomalies

MAG-anomalies of 40nT P2P value or higher were selected as archaeologically relevant to analyse. An SSS-anomaly was associated with a MAG-anomaly, if the distance between the two was 20 metres or less.

There was a significant difference in the number of MAG-targets in the OWF-area and the ECR-area, likely due to the magnetometer line spacing.

3.6.1. MAG-anomalies in the OWF-area

64 MAG-anomalies were selected in the OWF area. These anomalies are all included in the SSS-list above. 13 of these had no associated SSS-target.

3.6.2. MAG-anomalies in the ECR-area

245 MAG-anomalies were selected in the ECR-area. These anomalies automatically were all reviewed. Five large MAG-anomalies were given CONF 1 classification (see above) and all were reviewed and are included in the SSS-target list.

3.7. Conclusions regarding cultural historical archaeology

The archaeological analysis has reviewed all available data for the proposed OWF- and ECR-areas. In this geoarchaeological analysis it was possible to directly relate one target to a registered location in the OWF-area. This is the wreck of MS TOPSY. One registration in the ECR-area can be associated with MAG-anomalies, this association can be confirmed by diver surveys. These examples show how (un)reliable the available databases are and how they can only serve as guides for a geoarchaeological analysis.

The geoarchaeological analysis has revealed a lot of modern debris and fishing gear (CONF 4), as could be expected from the area.

The most important targets for a preliminary maritime archaeological survey excavation would be the diver and/or ROV-surveys of the anomalies classified as CONF 1 and CONF 2 targets.

The large MAG-targets associated with the FFM-registration are of outmost interest to maritime archaeology.

4. Conclusions

MAV has reviewed the data provided by Energinet and completed a desk-based geoarchaeological analysis of the geophysical survey. Based on the analyses, it is concluded that there is a reason to believe that there are protected Stone Age sites/material in the project area.

Furthermore, the large MAG-targets associated with the FFM-registration (KG_ECR2_MMO_PTS_1440,

KG_ECR_MMO_PTS_1441, KG_ECR2_MMO_PTS_1442, KG_ECR2_MMO_PTS_1443, KG_ECR2_MMO_PTS_1444) are of outmost interest to maritime archaeology.

5. Literature

- Andersen, S. H. (2005) “En glittestok fra Dogger Banke i Nordsøen”, *Kuml*, 54(54), s. 9–16. doi: 10.7146/kuml.v54i54.97309.
- Andersen, S. H. (2013) Tybrind Vig. Submerged Mesolithic settlements in Denmark.
- Astrup, P. M. 2018. *Sea-level change in Mesolithic southern Scandinavia. Long- and short-term effects on society and the environment*. Jutland Archaeological Society Publications Vol 106, 2018.
- Bendixen, C., Boldreel, L. O., Jensen, J. B., Bennike, O., Hübscher, C., & Clausen, O. R. (2017a). Early Holocene estuary development of the Hesselø Bay area, southern Kattegat, Denmark and its implication for Ancylus Lake drainage. Geo-Marine Letters, 37(6), 579–591. https://doi.org/10.1007/s00367-017-0513-7
- Bendixen, C., Jensen, J. B., Boldreel, L. O., Clausen, O. R., Bennike, O., Seidenkrantz, M.-S., Nyberg, J. & Hubscher, C. 2017b. The Holocene Great Belt connection to the southern Kattegat, Scandinavia: Ancylus Lake drainage and Early Littorina Sea transgression. *Boreas*. 10.1111/bor.12154. ISSN 0300-9483.
- Bennike, O., Jensen, J. B., Lemke, W., Kuijpers, A. & Lomholt, S. 2004. Late- and postglacial history of the Great Belt, Denmark. Boreas 33, 18–33.
- Bennike, O., Jensen. J. B., Nørgaard-Pedersen, N., Andresen. K. J., Seidenkrantz, M.-S., Moros, M. & Wagner, B. (2021). When were the straits between the Baltic Sea and the Kattegat inundated by the sea during the Holocene? *Boreas*. https://doi.org/10.1111/bor.12525.
- Björck, S. (1995). A review of the history of the Baltic Sea, 13.0-8.0 ka BP. Quaternary International,27, 19–40. https://doi.org/10.1016/1040-6182(94)00057-C
- Cohen, K. M. (2012). Regional chronostratigraphical correlation chart for the last 270,000 years: Europe north of the Mediterranean. Quaternary International, 279–280, 93–93. https://doi.org/10.1016/j.quaint.2012.07.410
- Coles, B. J. 1998. Doggerland: a Speculative Survey. *Proceedings of the Prehistoric Society* 64: 45-81.
- Dalicsek, D.P. 2023, Rapport: Kattegat Havvindmøllepark og kabelruter Arkæologisk analyse, Moesgård Museum
- Davidson, F. P. et al. (2011) Macro-engineering: MIT Brunel lectures on global infrastructure. Cambridge, England; Woodhead Publishing.
- Ehlers, J., Gibbard, P. L., & Hughes, P. D. (2011). Quaternary Glaciations - Extent and Chronology: A Closer Look: Vol. v.Volume 15 (1st ed.). Elsevier.
- Erlström, M., Kornfält, K.-A. & Sivhed, U. 2001: Berggrundskartan 2D Tomelilla NO/2E Simrishamn NV. Sveriges geologiska undersökning Af 213.
- Fairbanks, R.G. 1989, A 17,000-year glacio-eustatic sea level record: influnce of glacial melting rates on the Younger Dryas event and deep-ocean circulation. Nature, vol. 342, pp. 637-642.
- GEUS 2020: General geology of southern Kattegat, the Hesselø wind farm area. Desk Study. GEUS Rapport 2020/53.
- Gaffney, V., Allaby, R., Bates, R., Bates, M., Ch´ng, E., Fitch, S., Garwood, P., Momber, G., Murgatroyd, P., Pallen, M., Ramsey, E., Smith, D., Smith, O., 2017. Doggerland and the Lost Frontiers Project (2015-2020). In *Under the Sea: Archaeology and Palaeolandscapes of the*

Continental Shelf, eds. G. Bailey., J. Harff and D. Sakellariou, 305-309. Coastal Research Library.

- Gaffney, V., Thomson, K., and S. Fitch. 2007. *Mapping Doggerland. The Mesolithic Landscapes of the Southern North Sea*. Archaeopress.
- Heft, Tage: KLITFOLK: Langs Vestkysten fra Skagen til Sønderho. Alfred G. Hassings Forlag A/S, København 1941
- Hendriksen, Knud. VÅBEN I KLITTERNE – Noter om det tyske invasionsforsvar i Danmark 1940-45, Skive januar 1983
- Hohlenberg, J. (1885). Chart showing the strandings on the coasts of Denmark and on the Swedish coast between Marstrand and Carlskrona during the period from 1st January 1858 to 31st December 1885. Available at: http://www.kb.dk/maps/kortsa/2012/jul/kortatlas/object67921/da/ (Accessed 20 September 2022)
- Holt, Peter. (2019). Marine Magnetometer Processing, 3H Consulting Ltd
- Houmark-Nielsen, M., & Kjaer, K. (2003). Southwest Scandinavia, 40-15 kyr BP: palaeogeography and environmental change. Journal of Quaternary Science, 18(8), 769–786. https://doi.org/10.1002/jqs.802
- Houmark-Nielsen, M., Linge, H., Fabel, D., Schnabel, C., Xu, S., Wilcken, K.M. & Binnie, S. (2012). Cosmogenic surface exposure dating the last deglaciation in Denmark: discrepancies with independent age constraints suggest delayed periglacial landform stabilisation. Quaternary Geochronology 13, 1–17.
- Imray, James, Blachford, W., 1852, A new and improved chart of the North Sea or German Ocean, London, Available at: https://www.davidrumsey.com/luna/servlet/detail/RUMSEY~8~1~296993~90068582:A-new-and-improved-chart-of-the-Nor# Accessed: 04 October 2022
- James, M. et al. (2024). *Marine Geophysics: Data Acquisition, Processing, and Interpretation Guidance Notes (2nd Edition)*. Swindon. Historic England
- Jensen J. B., Petersen K. S., Konradi P., Kuijpers A., Bennike O., Lemke W., Endler R., (2002) Neotectonics, sea-level changes and biological evolution in the Fennoscandian border zone of the southern Kattegat Sea. Boreas 31:133–150. doi:10.1111/j.15023885.2002.tb01062.x
- Jensen, J. B., og Bennike, O., 2020. General geology of southern Kattegat, the Hesselø wind farm area. Report for Energinet Eltransmission A/S. Rapport 2020/53.
- Jensen, J. B., Bennike, O., Christensen, N. & Vangkilde-Pedersen, T. (2023). Screening of seabed geological conditions for the offshore wind farm area Kattegat and the adjacent cable corridor area. Desk study for Energinet. GEUS. Rapport 2023/33.
- Lambeck, K., Rouby, H., Purcell, Y.S. & Sambridge, M. 2014: Sea-level and global ice volumes from the Last Glacial Maximum to the Holocene. Proceedings of the National Academy of the United States of America (PNAS) 111, 15296–15303.
- Michael, C. (2011). *Magnetic Imaging of Shipwrecks*. University of Liverpool
- Reid, C. 1913. *Submerged Forests*. London: Cambridge University Press.
- Reimer, P. et al. 2020. The IntCal20 Northern Hemisphere radiocarbon age calibration curve (0-55 cal kB. Radiocarbon 62, doi: 10.1017/RDC.2020.41.
- Skriver, C., P.M. Astrup og P, Borup. 2018. Hjarnø Sund – all year, all inclusive. A submerged Late Mesolithic coastal site with organic remains. Journal of Danish Archaeology. pp. 1-23.

- Tarbensen Christensen, C. et al. (1995) De nærer sig af vrag: blandt strandfogeder, bjergere og redningsmænd imellem Nymindegab og Thorsminde. 1. oplag. Kbh: [Foreningen Danmarks Folkeminder].

6. Appendices

6.1. Table over CONF 1 and CONF 2 targets in the OWF area

TARGET_ID	COMMENT	MMO_TYPE	MAG_ANOMAL	SSS_ANOMAL	ARCH_CONF	ARCH_expl
25	Debris.	OD		KG_II_B01_SSS_GO5_0070	CONF 1	selected by NJK
27	Debris.	OD		KG_II_B01_SSS_GO5_0074	CONF 1	selected by NJK
28	Debris.	OD		KG_II_B01_SSS_GO5_0075	CONF 1	selected by NJK
32	Linear object. Possible rope fragment.	SR		KG_II_B01_SSS_GO5_0080	CONF 1	selected by NJK
33	Debris.	OD		KG_II_B01_SSS_GO5_0082	CONF 1	selected by NJK
102	Linear object. Possible rope fragment.	SR		KG_II_B01_SSS_GO5_0245	CONF 1	selected by NJK
393	Debris.	OD		KG_II_B02_SSS_GO5_0192	CONF 1	selected by NJK
395	Linear object. Possible rope fragment.	SR		KG_II_B02_SSS_GO5_0215	CONF 1	selected by NJK
396	Linear object. Possible rope fragment.	SR		KG_II_B02_SSS_GO5_0219	CONF 1	selected by NJK
400		DM	KG_II_B02_MAG_GO5_0011	KG_II_B02_SSS_GO5_0233	CONF 1	selected by NJK
401	Possible rope/wire/cable fragment.	OD		KG_II_B02_SSS_GO5_0235	CONF 1	selected by NJK
405	Possible cluster of metallic debris.	DM	KG_II_B02_MAG_GO5_0008	KG_II_B02_SSS_GO5_0273	CONF 1	MAG over 40nT, NJK
406	Possible cluster of metallic debris.	DM	KG_II_B02_MAG_GO5_0008	KG_II_B02_SSS_GO5_0275	CONF 1	MAG over 40nT, NJK
407	Debris.	OD		KG_II_B02_SSS_GO5_0296	CONF 1	selected by NJK
410	Possible cluster of metallic debris.	DM	KG_II_B02_MAG_GO5_0014	KG_II_B02_SSS_GO5_0303	CONF 1	selected by NJK
411	Possible cluster of metallic debris.	DM	KG_II_B02_MAG_GO5_0014	KG_II_B02_SSS_GO5_0305	CONF 1	selected by NJK
413		AN		KG_II_B02_SSS_GO5_0319	CONF 1	selected by NJK
422	Possible cluster of metallic debris.	DM	KG_II_B02_MAG_GO5_0025	KG_II_B02_SSS_GO5_0354	CONF 1	selected by NJK
423	Possible cluster of metallic debris.	DM	KG_II_B02_MAG_GO5_0025	KG_II_B02_SSS_GO5_0355	CONF 1	selected by NJK
431	Sonar Contact, within 10 m from targetKG_II_B02_MAG_GO5_0031.	OD		KG_II_B02_SSS_GO5_0417	CONF 1	selected by NJK
432	Possible cluster of metallic debris.	DM	KG_II_B02_MAG_GO5_0021	KG_II_B02_SSS_GO5_0419	CONF 1	selected by NJK
433	Possible cluster of metallic debris.	DM	KG_II_B02_MAG_GO5_0021	KG_II_B02_SSS_GO5_0420	CONF 1	selected by NJK
436	Sonar Contact, within 10 m from targetKG_II_B02_MAG_GO5_0033.	OD		KG_II_B02_SSS_GO5_0583	CONF 1	selected by NJK
462	Possible rope/wire fragment.	OD		KG_II_B02_SSS_GO5_1388	CONF 1	selected by NJK
463	Debris.	OD		KG_II_B02_SSS_GO5_1417	CONF 1	selected by NJK
489		DM	KG_II_B02_MAG_GO5_0075	KG_II_B02_SSS_GO5_1745	CONF 1	selected by NJK
512	Possible rope/wire/cable fragment.	OD		KG_II_B02_SSS_GO5_1825	CONF 1	selected by NJK
520	Debris.	AN		KG_II_B03_SSS_GO5_0581	CONF 1	selected by NJK
522	Debris.	OD		KG_II_B03_SSS_GO5_0595	CONF 1	selected by NJK
524	Debris.	OD		KG_II_B03_SSS_GO5_0605	CONF 1	selected by NJK
527	Debris.	OD		KG_II_B03_SSS_GO5_0612	CONF 1	selected by NJK
530	Debris.	OD		KG_II_B03_SSS_GO5_0617	CONF 1	selected by NJK
533	Linear object. Possible rope fragment.	SR		KG_II_B03_SSS_GO5_0744	CONF 1	selected by NJK
534	Debris.	OD		KG_II_B03_SSS_GO5_0747	CONF 1	selected by NJK
559		DM	KG_II_B03_MAG_GO5_0026	KG_II_B03_SSS_GO5_2178	CONF 1	MAG over 40nT, MMO, 447nT P2P
613		AN		KG_II_B04_SSS_GO5_0836	CONF 1	Anchor, low magnetism, 3,2x1,8m,admiralty stock type
679		DM	KG_II_B04_MAG_GO5_0071	KG_II_B04_SSS_GO5_1852	CONF 1	MAG over 40nT, NJK
764	Debris.	OD		KG_II_B04_SSS_GO5_7762	CONF 1	selected by NJK
765	Debris.	OD		KG_II_B04_SSS_GO5_7765	CONF 1	selected by NJK
770	Possible rope/wire fragment.	OD		KG_II_B05_SSS_GO5_0465	CONF 1	selected by NJK
800	Sonar Contact, within 10 m from targetKG_II_B05_MAG_GO6_0076.	OD		KG_II_B05_SSS_GO5_2027	CONF 1	selected by NJK
811		DM	KG_II_B05_MAG_GO6_0075	KG_II_B05_SSS_GO5_2513	CONF 1	selected by NJK
822	Possible rope/wire fragment.	OD		KG_II_B05_SSS_GO5_2774	CONF 1	selected by NJK

TARGET_ID	COMMENT	MMO_TYPE	MAG_ANOMAL	SSS_ANOMAL	ARCH_CONF	ARCH_expl
846	Debris.	OD		KG_II_B05_SSS_GO5_5639	CONF 1	selected by NJK
847	Debris.	OD		KG_II_B05_SSS_GO5_5640	CONF 1	selected by NJK
848	Debris.	OD		KG_II_B05_SSS_GO5_5641	CONF 1	selected by NJK
849	Debris.	OD		KG_II_B05_SSS_GO5_5642	CONF 1	selected by NJK
850	Debris.	OD		KG_II_B05_SSS_GO5_5643	CONF 1	selected by NJK
851	Debris.	OD		KG_II_B05_SSS_GO5_5644	CONF 1	selected by NJK
871	Debris.	OD		KG_II_B05_SSS_GO5_7489	CONF 1	selected by NJK
920	Sonar Contact, within 10 m from targetKG_II_B05_MAG_GO6_0081.	OD		KG_II_B05_SSS_GO5_7538	CONF 1	selected by NJK
939		DM	KG_II_B06_MAG_GO5_0004	KG_II_B06_SSS_GO5_5234	CONF 1	MAG over 40nT, NJK
949		DM	KG_II_B06_MAG_GO5_0015	KG_II_B06_SSS_GO5_5244	CONF 1	selected by NJK
952		DM	KG_II_B06_MAG_GO5_0018	KG_II_B06_SSS_GO5_5247	CONF 1	selected by NJK
954	Sonar Contact. Within 10m fromtarget KG_II_B06_MAG_G05_0004.	OD		KG_II_B06_SSS_GO5_5563	CONF 1	MAG over 40nT, NJK
956	Debris.	OD		KG_II_B07_SSS_GO5_1015	CONF 1	selected by NJK
985	Boulder	OD		KG_II_B04_SSS_GO5_2408	CONF 1	correlates with Ubåd 2526, MMO TARGET added by MAV
986	Boulder	OD		KG_II_B04_SSS_GO5_2409	CONF 1	correlates with Ubåd 2526, MMO TARGET added by MAV
987	Boulder	OD		KG_II_B04_SSS_GO5_2410	CONF 1	correlates with Ubåd 2526, MMO TARGET added by MAV
10		DM	KG_II_B01_MAG_GO6_0003	KG_II_B01_SSS_GO5_0036	CONF 2	Vragguide Ukendt 2535, see debris 9m south
11		DM	KG_II_B01_MAG_GO6_0004	KG_II_B01_SSS_GO5_0038	CONF 2	Vragguide Ukendt 2535, see neighbour, MAG under 40nT
13	Possible cluster of metallic debris.	DM	KG_II_B01_MAG_GO6_0010	KG_II_B01_SSS_GO5_0044	CONF 2	Odd shape high shadow, linear shape, stuck anchor?
41	Possible cluster of metallic debris.	DM	KG_II_B01_MAG_GO6_0027	KG_II_B01_SSS_GO5_0112	CONF 2	Ca. 21m long oval shape orientation NW-SE, shallow, 45m to NNE, ca.10 degrees
42	Possible cluster of metallic debris.	DM	KG_II_B01_MAG_GO6_0027	KG_II_B01_SSS_GO5_0113	CONF 2	Ca. 21m long oval shape orientation NW-SE, shallow, 45m to NNE, ca.10 degrees
43	Possible cluster of metallic debris.	DM	KG_II_B01_MAG_GO6_0027	KG_II_B01_SSS_GO5_0114	CONF 2	Ca. 21m long oval shape orientation NW-SE, shallow, 45m to NNE, ca.10 degrees
89	Debris.	OD		KG_II_B01_SSS_GO5_0192	CONF 2	Debris, non-metallic ODD SHAPE, LARGE, SMALL ANOMALIES NEARBY, DEPRESSION TOWARD WNW
125	Sonar Contact, within 10 m from targetKG_II_B01_MAG_GO6_0201.	OD		KG_II_B01_SSS_GO5_0439	CONF 2	SSS with MAG under 40nT, debris
126	Sonar Contact, within 10 m from targetKG_II_B01_MAG_GO6_0201.	OD		KG_II_B01_SSS_GO5_0443	CONF 2	SSS with MAG under 40nT, debris
153	Debris.	OD		KG_II_B01_SSS_GO5_0783	CONF 2	Debris, non-metallic
377	Possible cluster of metallic debris.	DM	KG_II_B01_MAG_GO6_0155	KG_II_B01_SSS_GO5_1703	CONF 2	Ca. 21m long oval shape orientation NW-SE, shallow, 36m to SSE, ca.160 degrees
378		OD		KG_II_B01_SSS_GO5_1704	CONF 2	Ca. 21m long oval shape orientation NW-SE, shallow, 36m to SSE, ca.160 degrees
519	Debris.	OD		KG_II_B03_SSS_GO5_0577	CONF 2	Debris, non-metallic,UNDISTURBED
588	Possible debris.	OD		KG_II_B03_SSS_GO5_2208	CONF 2	Linear 3m
655	Debris.	OD		KG_II_B04_SSS_GO5_1342	CONF 2	Debris, non-metallic, FURTHER DEBRIS 77M NORTHEAST
661	Debris.	OD		KG_II_B04_SSS_GO5_1458	CONF 2	Shallow/blurred contact, no specific indicators
677	Debris.	OD		KG_II_B04_SSS_GO5_1845	CONF 2	Debris, non-metallic
694	Debris.	OD		KG_II_B04_SSS_GO5_2171	CONF 2	Debris, non-metallic
703	Debris.	OD		KG_II_B04_SSS_GO5_2226	CONF 2	Debris, non-metallic
709	Debris.	OD		KG_II_B04_SSS_GO5_2251	CONF 2	Debris, non-metallic
710	Debris.	OD		KG_II_B04_SSS_GO5_2252	CONF 2	Debris, non-metallic
719	Debris.	OD		KG_II_B04_SSS_GO5_2324	CONF 2	Debris, non-metallic
720	Debris.	OD		KG_II_B04_SSS_GO5_2341	CONF 2	Debris, non-metallic MMO
722	Debris.	OD		KG_II_B04_SSS_GO5_2398	CONF 2	Debris, non-metallic, SEE OBJECT 65M TO NNW

TARGET_ID	COMMENT	MMO_TYPE	MAG_ANOMAL	SSS_ANOMAL	ARCH_CONF	ARCH_expl
727		DM	KG_II_B04_MAG_GO5_0083	KG_II_B04_SSS_GO5_2569	CONF 2	MAG over 40nT DEBRIS
728	Debris.	OD		KG_II_B04_SSS_GO5_2584	CONF 2	Debris, non-metallic
730	Debris.	OD		KG_II_B04_SSS_GO5_2702	CONF 2	Debris, non-metallic
732	Debris.	OD		KG_II_B04_SSS_GO5_2907	CONF 2	Debris, non-metallic
734	Debris.	OD		KG_II_B04_SSS_GO5_3032	CONF 2	Debris, non-metallic
736	Debris.	OD		KG_II_B04_SSS_GO5_3172	CONF 2	Debris, non-metallic
738	Debris.	OD		KG_II_B04_SSS_GO5_3215	CONF 2	Debris, non-metallic
740	Debris.	OD		KG_II_B04_SSS_GO5_3238	CONF 2	DEBRIS
742	Linear object.	OD		KG_II_B04_SSS_GO5_3273	CONF 2	Debris
752	Debris.	OD		KG_II_B04_SSS_GO5_4485	CONF 2	Debris, non-metallic
756	Debris.	OD		KG_II_B04_SSS_GO5_4567	CONF 2	Debris, non-metallic
772	Debris.	OD		KG_II_B05_SSS_GO5_0730	CONF 2	Debris, non-metallic LINEAR
773	Debris.	OD		KG_II_B05_SSS_GO5_0740	CONF 2	Debris, non-metallic
776	Debris.	OD		KG_II_B05_SSS_GO5_0961	CONF 2	Debris, non-metallic
780	Debris.	OD		KG_II_B05_SSS_GO5_1235	CONF 2	Debris, non-metallic
782	Debris.	OD		KG_II_B05_SSS_GO5_1528	CONF 2	Debris, non-metallic
785	Sonar Contact.	OD		KG_II_B05_SSS_GO5_1804	CONF 2	Debris LINEAR
787	Sonar Contact.	OD		KG_II_B05_SSS_GO5_1806	CONF 2	Debris
788	Sonar Contact.	OD		KG_II_B05_SSS_GO5_1807	CONF 2	Debris
798	Sonar Contact.	OD		KG_II_B05_SSS_GO5_1817	CONF 2	Debris
815	Sonar Contact.	OD		KG_II_B05_SSS_GO5_2526	CONF 2	Debris
819	Sonar Contact.	OD		KG_II_B05_SSS_GO5_2530	CONF 2	Debris
821	Debris.	OD		KG_II_B05_SSS_GO5_2762	CONF 2	Debris, non-metallic
823	Debris.	OD		KG_II_B05_SSS_GO5_2991	CONF 2	Debris, non-metallic
824	Debris.	OD		KG_II_B05_SSS_GO5_3163	CONF 2	Debris, non-metallic
838	Sonar Contact.	OD		KG_II_B05_SSS_GO5_4778	CONF 2	Debris
854	Sonar Contact.	OD		KG_II_B05_SSS_GO5_5663	CONF 2	Debris
855	Debris.	OD		KG_II_B05_SSS_GO5_5700	CONF 2	Debris, non-metallic
856	Debris.	OD		KG_II_B05_SSS_GO5_5732	CONF 2	Debris
858	Debris.	OD		KG_II_B05_SSS_GO5_6055	CONF 2	Debris, non-metallic LINEAR
869	Debris.	OD		KG_II_B05_SSS_GO5_7435	CONF 2	Debris, non-metallic
889		DM	KG_II_B05_MAG_GO6_0024	KG_II_B05_SSS_GO5_7507	CONF 2	MAG over 40nT, STRONG MAGNETISM
923	Debris.	OD		KG_II_B06_SSS_GO5_0124	CONF 2	Debris, non-metallic
925	Debris.	OD		KG_II_B06_SSS_GO5_0169	CONF 2	Debris, non-metallic
927	Debris.	OD		KG_II_B06_SSS_GO5_2016	CONF 2	Debris, non-metallic
930	Debris.	OD		KG_II_B06_SSS_GO5_2622	CONF 2	Debris, non-metallic
931	Debris.	OD		KG_II_B06_SSS_GO5_4169	CONF 2	Debris, non-metallic
932	Debris.	OD		KG_II_B06_SSS_GO5_4314	CONF 2	Debris, non-metallic
963	Debris.	OD		KG_II_B07_SSS_GO5_1658	CONF 2	Debris, non-metallic
560	Sonar Contact, within 10 m from targetKG_II_B03_MAG_GO5_0029.	OD		KG_II_B03_SSS_GO5_2179	CONF 2	Shallow/blurred contact, no specific indicators
561	Sonar Contact, within 10 m from targetKG_II_B03_MAG_GO5_0029.	OD		KG_II_B03_SSS_GO5_2180	CONF 2	Shallow/blurred contact, no specific indicators
562	Sonar Contact, within 10 m from targetKG_II_B03_MAG_GO5_0029.	OD		KG_II_B03_SSS_GO5_2181	CONF 2	Shallow/blurred contact, no specific indicators

6.2. Table over CONF 1 and CONF 2 targets in the ECR area

TARGETID	COMMENT	MMO_TYPE	MAG_ANOMAL	SSS_ANOMAL	ARCH_CONF	ARCH_expl
KG_ECR2_MMO_PTS_0552	Sonar Contact. Within 10 metres from MAG target KG_ECR2-A_MAG_GO4_0546.	OD		KG_ECR2A_SSS_GO4_0324	CONF 1	Dragged object/anchor
KG_ECR2_MMO_PTS_0702	Sonar Contact. Within 10 metres from MAG targets KG_ECR2-A_MAG_GO4_0636 KG_ECR2-A_MAG_GS17_0633 KG_ECR2-A_MAG_GS17_0638.	AN		KG_ECR2A_SSS_GS17_0094	CONF 1	MAG over 40nT, ANCHOR
KG_ECR2_MMO_PTS_0703		AN	KG_ECR2-A_MAG_GO4_0636 KG_ECR2-A_MAG_GS17_0633 KG_ECR2-A_MAG_GS17_0638	KG_ECR2A_SSS_GS17_0095	CONF 1	MAG over 40nT, ANCHOR
KG_ECR2_MMO_PTS_0968		AN		KG_ECR2B_SSS_GO4_0216	CONF 1	ANCHOR
KG_ECR2_MMO_PTS_1074		DM	KG_ECR2-B_MAG_GO4_0895	KG_ECR2B_SSS_GO4_0322	CONF 1	MAG over 40nT, wreck?
KG_ECR2_MMO_PTS_1076		DM	KG_ECR2-B_MAG_GO4_0896	KG_ECR2B_SSS_GO4_0324	CONF 1	MAG over 40nT, wreck?
KG_ECR2_MMO_PTS_1077		DM	KG_ECR2-B_MAG_GO4_0898	KG_ECR2B_SSS_GO4_0325	CONF 1	wreck?
KG_ECR2_MMO_PTS_1136	Debris.	DN		KG_ECR2B_SSS_GO4_0384	CONF 1	ASS WITH ANCHOR
KG_ECR2_MMO_PTS_1137		DM	KG_ECR2-B_MAG_GO4_0935	KG_ECR2B_SSS_GO4_0385	CONF 1	ASS WITH ANCHOR
KG_ECR2_MMO_PTS_1138	Linear object.	DN		KG_ECR2B_SSS_GO4_0386	CONF 1	ANCHOR
KG_ECR2_MMO_PTS_1153	Sonar Contact. Within 10 metres from MAG target KG_ECR2-B_MAG_GO4_0941.	AN	KG_ECR2-B_MAG_GO4_0941	KG_ECR2B_SSS_GO4_0401	CONF 1	ANCHOR
KG_ECR2_MMO_PTS_1154	Linear object. Sonar Contact. Within 10 metres from MAG target KG_ECR2-B_MAG_GO4_0941. Possible cable/wire fragment. Length measurement is not accurate. For correct length please refer to MMO Linear shp.	OD		KG_ECR2B_SSS_GO4_0402	CONF 1	fishing gear ass w anchor
KG_ECR2_MMO_PTS_1304		AN	KG_ECR2-B_MAG_GO4_1029	KG_ECR2B_SSS_GO4_0552	CONF 1	ANCHOR
KG_ECR2_MMO_PTS_1440	large MAG anomaly, FFM association, shipwreck?	ARCH	KG_ECR2-A_MAG_GSV_0005		CONF 1	large MAG anomaly, FFM association, shipwreck?,FFM within 200m
KG_ECR_MMO_PTS_1441		ARCH	KG_ECR2-A_MAG_GSV_0002		CONF 1	large MAG, FFM ass., shipwreck?,FFM within 200m
KG_ECR2_MMO_PTS_1442		ARCH	KG_ECR2-A_MAG_GSV_0001		CONF 1	large MAG, FFM ass., shipwreck?,FFM within 200m
KG_ECR2_MMO_PTS_1443		ARCH	KG_ECR2-A_MAG_GSV_0004		CONF 1	large MAG, FFM ass., shipwreck?,FFM within 200m
KG_ECR2_MMO_PTS_1444		ARCH	KG_ECR2-A_MAG_GSV_0003		CONF 1	large MAG, FFM ass, shipwreck?,FFM within 200m
KG_ECR2_MMO_PTS_0004		DM	KG_ECR2-A_MAG_GeoX_0016	KG_ECR2A_SSS_GEOX_0004	CONF 2	MAG over 40nT
KG_ECR2_MMO_PTS_0005	Debris.	DN		KG_ECR2A_SSS_GEOX_0005	CONF 2	MAG over 40nT

TARGETID	COMMENT	MMO_TYPE	MAG_ANOMAL	SSS_ANOMAL	ARCH_CONF	ARCH_expl
KG_ECR2_MMO_PTS_0024		DM	KG_ECR2-A_MAG_GeoX_0028	KG_ECR2A_SSS_GEOX_0025	CONF 2	MAG over 40nT, CLOSE TO ffm
KG_ECR2_MMO_PTS_0032		DM	KG_ECR2-A_MAG_GS17_0041	KG_ECR2A_SSS_GEOX_0034	CONF 2	MAG over 40nT
KG_ECR2_MMO_PTS_0035		DM	KG_ECR2-A_MAG_GeoX_0043	KG_ECR2A_SSS_GEOX_0037	CONF 2	MAG over 40nT,FFM within 200m
KG_ECR2_MMO_PTS_0036		DM	KG_ECR2-A_MAG_GeoX_0044	KG_ECR2A_SSS_GEOX_0038	CONF 2	MAG over 40nT,FFM within 200m
KG_ECR2_MMO_PTS_0069		DM	KG_ECR2-A_MAG_GeoX_0073	KG_ECR2A_SSS_GEOX_0071	CONF 2	MAG over 40nT, SHALLOW LINEAR
KG_ECR2_MMO_PTS_0081	Possible cluster of metallic debris.	DM	KG_ECR2-A_MAG_GeoX_0082	KG_ECR2A_SSS_GEOX_0083	CONF 2	MAG over 40nT, LARGE OBJECT 20M TO NORTHEAST
KG_ECR2_MMO_PTS_0094		DM	KG_ECR2-A_MAG_GeoX_0092	KG_ECR2A_SSS_GEOX_0096	CONF 2	MAG over 40nT
KG_ECR2_MMO_PTS_0097	Debris.	DN		KG_ECR2A_SSS_GEOX_0099	CONF 2	MAG over 40nT, LARGE LINEAR OBJECT
KG_ECR2_MMO_PTS_0166		DM	KG_ECR2-A_MAG_GeoX_0189	KG_ECR2A_SSS_GEOX_0169	CONF 2	MAG over 40nT, COVERED DEBRIS
KG_ECR2_MMO_PTS_0250		DM	KG_ECR2-A_MAG_GS17_0228	KG_ECR2A_SSS_GO4_0021	CONF 2	MAG over 40nT, DEBRIS, NO TRACKS
KG_ECR2_MMO_PTS_0255		DM	KG_ECR2-A_MAG_GeoX_0229	KG_ECR2A_SSS_GO4_0026	CONF 2	MAG over 40nT, DEBRIS NO RECENT TRACKS
KG_ECR2_MMO_PTS_0319		DM	KG_ECR2-A_MAG_GeoX_0311	KG_ECR2A_SSS_GO4_0090	CONF 2	MAG over 40nT, DEBRIS WO RECENT TRACKS
KG_ECR2_MMO_PTS_0320		DM	KG_ECR2-A_MAG_GO4_0313	KG_ECR2A_SSS_GO4_0091	CONF 2	MAG over 40nT, SEDIMENT MOUND
KG_ECR2_MMO_PTS_0322	Possible cluster of metallic debris.	DM	KG_ECR2-A_MAG_GO4_0317	KG_ECR2A_SSS_GO4_0093	CONF 2	MAG over 40nT, SEDIMENT MOUND
KG_ECR2_MMO_PTS_0323		DM	KG_ECR2-A_MAG_GO4_0329 KG_ECR2-A_MAG_GO4_0330	KG_ECR2A_SSS_GO4_0094	CONF 2	MAG over 40nT, MMO, NO RECENT TRACKS
KG_ECR2_MMO_PTS_0324		DM	KG_ECR2-A_MAG_GeoX_0318	KG_ECR2A_SSS_GO4_0095	CONF 2	MAG over 40nT, STRAIGHT LINE HIGH SHADOW
KG_ECR2_MMO_PTS_0334		DM	KG_ECR2-A_MAG_GO4_0337	KG_ECR2A_SSS_GO4_0105	CONF 2	MAG over 40nT, COMPLEX OBJ
KG_ECR2_MMO_PTS_0340	Possible cluster of metallic debris.	DM	KG_ECR2-A_MAG_GO4_0334	KG_ECR2A_SSS_GO4_0111	CONF 2	MAG over 40nT, LINEAR MMO
KG_ECR2_MMO_PTS_0362	Sonar Contact. Within 10 metres from MAG target KG_ECR2-A_MAG_GO4_0363.	OD		KG_ECR2A_SSS_GO4_0134	CONF 2	anomalies/anomaly shapes in a row, shallow
KG_ECR2_MMO_PTS_0372	Linear object.	DN		KG_ECR2A_SSS_GO4_0144	CONF 2	solid linear obj
KG_ECR2_MMO_PTS_0376	Linear object.	DN		KG_ECR2A_SSS_GO4_0148	CONF 2	solid linear obj
KG_ECR2_MMO_PTS_0396		DM	KG_ECR2-A_MAG_GeoX_0389	KG_ECR2A_SSS_GO4_0168	CONF 2	MAG over 40nT, MMO LINEAR OBJ
KG_ECR2_MMO_PTS_0539	Possible cluster of metallic debris.	DM	KG_ECR2-A_MAG_GO4_0533	KG_ECR2A_SSS_GO4_0311	CONF 2	MAG over 40nT
KG_ECR2_MMO_PTS_0547		DM	KG_ECR2-A_MAG_GS17_0540	KG_ECR2A_SSS_GO4_0319	CONF 2	MAG over 40nT
KG_ECR2_MMO_PTS_0550		DM	KG_ECR2-A_MAG_GO4_0544	KG_ECR2A_SSS_GO4_0322	CONF 2	MAG over 40nT ASS WITH ANCHOR

TARGETID	COMMENT	MMO_TYPE	MAG_ANOMAL	SSS_ANOMAL	ARCH_CONF	ARCH_expl
KG_ECR2_MMO_PTS_0555	Possible cluster of metallic debris.	DM	KG_ECR2-A_MAG_GO4_0550	KG_ECR2A_SSS_GO4_0327	CONF 2	ASS WITH ANCHOR
KG_ECR2_MMO_PTS_0595		DM	KG_ECR2-A_MAG_GS17_0609	KG_ECR2A_SSS_GO4_0367	CONF 2	MAG over 40nT, RECTANGULAR
KG_ECR2_MMO_PTS_0597		DM	KG_ECR2-A_MAG_GO4_0610	KG_ECR2A_SSS_GO4_0369	CONF 2	MAG over 40nT, MMO
KG_ECR2_MMO_PTS_0680		DM	KG_ECR2-A_MAG_GO4_0534	KG_ECR2A_SSS_GS17_0072	CONF 2	MAG over 40nT, COMPLEX
KG_ECR2_MMO_PTS_0704		DM	KG_ECR2-A_MAG_GS17_0642	KG_ECR2A_SSS_GS17_0096	CONF 2	MAG over 40nT
KG_ECR2_MMO_PTS_0736		DM	KG_ECR2-A_MAG_GS17_0743	KG_ECR2A_SSS_GS17_0130	CONF 2	MAG over 40nT, MMO
KG_ECR2_MMO_PTS_0821	Possible cluster of metallic debris.	DM	KG_ECR2-B_MAG_GO4_0745	KG_ECR2B_SSS_GO4_0069	CONF 2	MAG over 40nT, LINEAR MMO
KG_ECR2_MMO_PTS_0848	Linear object.	DN		KG_ECR2B_SSS_GO4_0096	CONF 2	MMO features, ANCHOR
KG_ECR2_MMO_PTS_0874		DM	KG_ECR2-B_MAG_GO4_0782	KG_ECR2B_SSS_GO4_0122	CONF 2	MAG over 40nT, SHARP SHADOW
KG_ECR2_MMO_PTS_0891		DM	KG_ECR2-B_MAG_GO4_0797	KG_ECR2B_SSS_GO4_0139	CONF 2	MAG over 40nT, COMPLEX.MMO
KG_ECR2_MMO_PTS_0925	Debris field.	DM	KG_ECR2-B_MAG_GO4_0814 KG_ECR2-B_MAG_GO4_0815 KG_ECR2-B_MAG_GO4_0816	KG_ECR2B_SSS_GO4_0173	CONF 2	MAG over 40nT, DEBRIS
KG_ECR2_MMO_PTS_0927	Debris field.	DN		KG_ECR2B_SSS_GO4_0175	CONF 2	Debris
KG_ECR2_MMO_PTS_0959		DM	KG_ECR2-B_MAG_GO4_0829	KG_ECR2B_SSS_GO4_0207	CONF 2	Debris, ass with solid linear feature
KG_ECR2_MMO_PTS_0963	Linear object.	DN		KG_ECR2B_SSS_GO4_0211	CONF 2	Debris, ass with solid linear feature
KG_ECR2_MMO_PTS_0964	Debris.	DN		KG_ECR2B_SSS_GO4_0212	CONF 2	Debris, ass with solid linear feature
KG_ECR2_MMO_PTS_0999		DM	KG_ECR2-B_MAG_GO4_0847	KG_ECR2B_SSS_GO4_0247	CONF 2	MAG over 40nT, MMO
KG_ECR2_MMO_PTS_1012	Sonar Contact. Within 10 metres from MAG target KG_ECR2-B_MAG_GO4_0854.	OD		KG_ECR2B_SSS_GO4_0260	CONF 2	Close to MAG over 40nT, linear shape
KG_ECR2_MMO_PTS_1014		DM	KG_ECR2-B_MAG_GO4_0856	KG_ECR2B_SSS_GO4_0262	CONF 2	MAG over 40nT, MMO
KG_ECR2_MMO_PTS_1305	Possible cluster of metallic debris.	DM	KG_ECR2-B_MAG_GO4_1031	KG_ECR2B_SSS_GO4_0553	CONF 2	MAG over 40nT, LINEAR, DEBRIS, MAYBE ANCHOR
KG_ECR2-B_MAG_GO4_0762	MAG anomaly with unmarked SSS contact 275nT	DM	KG_ECR2-B_MAG_GO4_0762		CONF 2	MAG anomaly with unmarked SSS contact 275nT

6.3. SLIPs from the Hesselø South OWF and Kattegat OWF and ECR areas

EUREF 89 N	EUREF 89 E	lab_nr	Nr.	site	sample	C14 age uncal. BP	Uncertainty	correction	corrected age	Elevation	sediment cover above sample	OxCal code
6293731,25	674484,15	AAR-1576	1	Kattegat, corring, PC 10-07	Marine shells,	8840	75	400	8440	-53,20	3,22	R_Date("1", 8440, 75) {z=-53.20;color="blue"};
6242857,42	663248,37	AAR-1332	2	Kattegat, corring, K1	Marine shells,	6780	120	400	6380	-32,45	2,46	R_Date("2", 6380, 120){z=-32.45;color="blue"};
6236309,70	694830,10	AAR-1088	3	Kattegat, corring, Psh 2981	Marine shells, Cardium	9030	100	400	8630	-27,11	3,11	R_Date("3", 8630, 100){z=-27.11;color="blue"};
6236309,70	694830,10	AAR-1086	4	Kattegat, corring, Psh 2981	Marine shells,	9340	160	400	8940	-24,80	0,80	R_Date("4", 8940, 160){z=-24.80;color="blue"};
6276885,82	672672,14	AAR-3042	5	Kattegat, corring, 572004	Marine shells, Mytilus Edulis	10120	75	400	9720	-25,30	3,50	R_Date("5", 9720, 75) {z=-25.30;color="blue"};
6276885,82	672672,14	AAR-3043	6	Kattegat, corring, 572004	Marine shells, Astarte Borealis	11930	100	400	11530	-39,47	5,57	R_Date("6", 11530, 100){z=-39.47;color="blue"};
6277650,91	673488,70	AAR-5058	7	Kattegat, corring, 572003	Marine shells, Portlandia Arctica	13070	100	400	12670	-39,00	5,70	R_Date("7", 12670, 100){z=-39.00;color="blue"};
6293731,25	674484,15	AAR-1575	8	Kattegat, corring, PC 10-07	Marine shells, Arctica islandica	11050	100	400	10650	-56,66	6,66	R_Date("8", 10650, 100){z=-56.66;color="blue"};
6232077,30	652994,77	St-2174	9	Kattegat, core B 504	Peat	9725	200	0	9725	-22,00	1,00	R_Date("9", 9725, 200){z=-22.00;color="green"};
6252192,83	700046,45	Ua-91	10	Kattegat, core 8533	Marine shells, Macoma Calcarrea	12450	170	400	12050	-37,60	4,12	R_Date("10", 12050, 170){z=-37.60;color="blue"};
6252207,96	661067,02	AAR-3041	11	Kattegat, core 572002	Marine shells, Macoma baltica	9750	65	400	9350	-30,60	4,50	R_Date("11", 9350, 65){z=-30.60;color="blue"};
6260098,90	664351,86	AAR-4063	12	Kattegat, core no. 572012	Marine shells, Cerastoderma edule	9145	75	400	8745	-33,35	5,25	R_Date("12", 8745, 75){z=-33.35;color="blue"};
6260098,90	664351,86	AAR-4062	13	Kattegat, core no. 572012	Marine shells, Balanus crenatus, Cerastoderma edule	8520	55	400	8120	-28,70	0,60	R_Date("13", 8120, 55){z=-28.70;color="blue"};
6260144,24	663655,46	AAR-4061	14	Kattegat, core no. 212640	Marine shells, Cerastoderma edule, Macoma balthica	9235	55	400	8835	-30,20	2,30	R_Date("14", 8835, 55){z=-30.20;color="blue"};
6260458,27	653706,59	AAR-4537	16	Kattegat	Marine shells, Macoma baltica	9960	90	400	9560	-30,50	4,85	R_Date("16", 9560, 90){z=-30.50;color="blue"};
6236168,40	689796,93	AAR-5132	17	Kattegat	Marine shells, Portlandia arctica	13310	90	400	12910	-29,75	2,85	R_Date("17", 12910, 90){z=-29.75;color="blue"};
6235602,27	690657,11	AAR-5131	18	Kattegat	Marine shells, Macoma balthica	11040	60	400	10640	-29,03	2,50	R_Date("18", 10640, 60){z=-29.03;color="blue"};
6272681,59	660188,32	AAR-4527	19	Kattegat	Marine shells, Macoma baltica	13070	100	400	12670	-32,00	3,00	R_Date("19", 12640, 100){z=-32.0;color="blue"};
6272681,59	660188,32	AAR-4527.1	21	Kattegat	Marine shells, Macoma baltica	13670	110	400	13270	-32,00	3,00	R_Date("21", 13270, 110){z=-32.00;color="blue"};
6260458,27	653706,59	AAR-4536	22	Kattegat	Marine shells, Mytilus edulis	9600	80	400	9200	-29,00	3,20	R_Date("22", 9200, 80){z=-29.00;color="blue"};
6260144,96	663662,35	AAR-4535	23	Kattegat, core no 572011	Marine shells, Mytilus edulis	10050	90	400	9650	-33,50	5,55	R_Date("23", 9650, 90){z=-33.50;color="blue"};
6252207,96	661067,02	AAR-4532	24	Kattegat, core no 572002	Marine shells, Mya truncata	8730	90	400	8330	-23,20	1,40	R_Date("24", 8330, 90){z=-23.20;color="blue"};
6261276,60	652969,19	AAR-4526	25	Kattegat, corring, 572017	Marine shells, Hiatella Arctica	14000	120	400	13600	-32,72	5,00	R_Date("25", 13600, 100){z=-32.72;color="blue"};

EUREF 89 N	EUREF 89 E	lab_nr	Nr.	site	sample	C14 age uncal. BP	Uncertainty	correction	corrected age	Elevation	sediment cover above sample	OxCal code
6252207,96	661067,02	AAR-4531	26	Kattegat, core no 572002	Marine shells, Corbula gibba	8340	80	400	7940	-22,80	1,00	R_Date("26", 7940, 80){z=-22.80;color="blue"};
6231348,30	683047,30	St-2171	27	Northern zealand	Peat	10820	200	0	10820	-26,70	1,70	R_Date("27", 10820, 200){z=-26.70;color="green"};
6267076,87	658476,72	AAR-4534	28	Kattegat, corring, 572009	Marine shells, Mytilus Edulis	10410	80	400	10010	-34,15	4,95	R_Date("28", 10010, 80){z=-34.15;color="blue"};
6267076,87	658476,72	AAR-4533	29	Kattegat, corring, 572009	Marine shells, Mytilus Edulis	10310	80	400	9910	-32,85	3,65	R_Date("29", 9910, 80){z=-32.85;color="blue"};
6267076,00	658476,72	K-6959	30	Kattegat, corring, 572009	Marine shells, Cerastoderma edule	9010	120	0	9022	-30,00	0,80	R_Date("30", 9022, 120){z=-30;color="blue"};
6261449,00	668702,00	Beta-585279	31	Hesselø, 5.2D, VC_15	Marine shells, Littorina	10060	30	400	9660	-33,90		R_Date("31", 9660, 30){z=-33.90;color="blue"};
6235402,00	692572,00	Beta-585280	32	Hesselø, 4.2D, GL03_14	Marine shells, Littorina	9790	30	400	9390	-30,00		R_Date("32", 9390, 30){z=-30.00;color="blue"};
6249604,00	673430,00	Beta-585281	33	Hesselø, 3.2D, GL06_05	Marine shells, Cerastoderma	9760	30	400	9360	-30,30		R_Date("33", 9360, 30){z=-30.30;color="blue"};
6236101,00	691845,00	Beta-585282	34	Hesselø, 3.3D, GL04_1A	Marine shells, Cerastoderma	9960	30	400	9560	-30,60		R_Date("34", 9560, 30){z=-30.60;color="blue"};
6274534,00	675206,00	Beta-585283	35	Hesselø, 2.2D, VC_02	Marine shells, Cerastoderma	7970	30	400	7570	-32,50		R_Date("35", 7570, 30){z=-32.50;color="blue"};
6256737,00	665264,00	Beta-585284	36	Hesselø, 2.3D, VC_23A	Plant material, twig	9020	30	400	8620	-30,60		R_Date("36", 8620, 30){z=-30.60;color="blue"};
6254849,00	663128,00	Beta-473575	38	MSM22	Marine shells	10260	30	400	9860	-35,60		R_Date("38", 9860, 30){z=-35.60;color="blue"};
6226633,32	650223,02	AAR-8841	39	core 258030	Marine shells	8275	65	400	7875	-28,30		R_Date("39", 7875, 65){z=-28.30;color="blue"};
6226633,32	650223,02	AAR-8840	40	core 258030	Marine shells	8410	80	400	8010	-30,60		R_Date("40", 8010, 80){z=-30.60;color="blue"};
6254943.10	646012,28	AAR-38173	41	Kattegat, KG 02 - P03 (B2) X8	Marine shells (sand with shell fragments)	4230	31	400	3830	-28,37	2,77	R_Date("41", 3830, 31){z=-28.37;color="blue"};
6251784.23	640259,76	AAR-38169	42	Kattegat, KG 07 - P01 (B1) X9	Marine shells (Clay with shell fragments)	4207	34	400	3807	-21,32	0,8	R_Date("42", 3807, 34){z=-21.32;color="blue"};
6251784.23	640259,76	AAR-38168	43	Kattegat, KG 07 - P01 (B2) X7	Marine shells (Clay with shell fragments)	2129	30	400	1729	-21,62	1,1	R_Date("43", 1729, 30){z=-21.62;color="blue"};
6249427.53	643640,64	AAR-38170	44	Kattegat, KG 12 - P03 (B2) X4	Marine shells (sand with shell fragments)	7538	44	400	7138	-21,09	2,66	R_Date("44", 7138, 44){z=-21.09;color="blue"};
6240084.01	634461,71	AAR-38172	45	Kattegat, KG 25 - P01 (B2) X10	Marine shells (sand with shell fragments)	4815	32	400	4415	-21,54	0,66	R_Date("45", 4415, 32){z=-21.54;color="blue"};
6240084,01	634461,71	AAR-38171	46	Kattegat, KG 25 - P01 (B2) X11	Hazelnut/nutshell (sand)	8871	45	0	8871	-21,54	0,66	R_Date("46", 8871, 45){z=-21.54;color="blue"};
6240084,01	634461,71	AAR-38166	47	Kattegat, KG 25 - P02 (B2) X5	Marine shells (organic material)	4545	42	400	4145	-22,29	1,39	R_Date("47", 4145, 42){z=-22.29;color="blue"};
6240084,01	634461,71	AAR-38167	48	Kattegat, KG 25 - P02 (B2) X6	Wood (organic material)	9148	53	0	9148	-22,29	1,39	R_Date("48", 9148, 53){z=-22.29;color="blue"};
6252621,00	670303,40	AAR-38165	49	Hesselø, HS 06 - P2 (B3) X1	Cardium shell (clay)	9057	48	400	8657	-29,87	4,99	R_Date("49", 8657, 48){z=-29.87;color="blue"};
6250566,90	664070,40	AAR-38163	50	Hesselø, HS 11 - P2 (B1) X3	Marine shells (sand with shell fragments)	9101	42	400	8701	-32,69	4,38	R_Date("50", 8701, 42){z=-32.59;color="blue"};

EUREF 89 N	EUREF 89 E	lab_nr	Nr.	site	sample	C14 age uncal. BP	Uncertainty	correction	corrected age	Elevation	sediment cover above sample	OxCal code
6250566,90	664070,40	AAR-38164	51	Hesselø, HS 11 - P2 (B1) X2	Wood (sand)	8861	50	0	8861	-32,69	4,38	R_Date("51", 8861, 50){z=-32.69;color="blue"};
6241607,27	596152,98	K-3987	52	Korupsø, well 1	Marine shells, Mytilus edulis, Cardium edulis	4910	90	0	4910	-5,5		R_Date("52", 4910, 90){z=-5.5;color="blue"};
6241607,27	596152,98	K-3988	53	Korupsø, well 1	Marine shells, Corbula gibba	7240	110	0	7240	-8,5		R_Date("53", 7240, 110){z=-8.75;color="blue"};
6241607,27	596152,98	K-3989	54	Korupsø, well 1	Marine shells, Cardium edulis	7370	110	0	7370	-8,7		R_Date("54", 7370, 110){z=-8.70;color="blue"};
6241607,27	596152,98	K-3990	55	Korupsø, well 1	Marine shells, Corbula gibba	7380	110	0	7380	-8,7		R_Date("55", 7380, 110){z=-8.70;color="blue"};
6241607,27	596152,98	K-4235	56	Korupsø, well 2	Marine shells, Mytilus edulis	6750	100	0	6750	-4,4		R_Date("56", 6750, 100){z=-4.40;color="blue"};
6241607,27	596152,98	K-4236	57	Korupsø, well 2	Marine shells, Ostrea edulis	6990	100	0	6990	-4,5		R_Date("57", 6990, 100){z=-4.50;color="blue"};
6241607,27	596152,98	K-4237	58	Korupsø, well 2	Marine shells, Mytilus edulis and cardium edulis	7990	100	0	7990	-5,5		R_Date("58", 7990, 100){z=-5.50;color="blue"};
6231469,14	585912,11	AAR-8415	59	Kalø Vig I, coastal settlement, refuse layer	Wood, fishing pole	7550	40	0	7550	-6,4		R_Date("59", 7550, 40){z=-6.40;color="grey"};
6231469,14	585912,11	AAR-27407	60	Kalø Vig I, coastal settlement, refuse layer	Wood, burnt branch	7563	49	0	7563	-7,6		R_Date("60", 7563, 49){z=-7.60;color="grey"};
6231469,14	585912,11	AAR-24408	61	Kalø Vig I, coastal settlement, refuse layer	Wood, burnt branch	7739	41	0	7739	-7,6		R_Date("61", 7739, 41){z=-7.60;color="grey"};
6231469,14	585912,11	AAR-27412	62	Kalø Vig I, coastal settlement, tree stump	Tree stump	7813	75	0	7813	-7,2		R_Date("62", 7813, 75){z=-7.20;color="green"};
6264786,95	600037,99	AAR-13398	63	Jesholm 1, coastal settlement, refuse layer	Wood, trunk	6983	45	0	6983	2,85		R_Date("63", 6983, 45){z=-2.85;color="grey"};
6264786,95	600037,99	AAR-13399	64	Jesholm 1, coastal settlement, refuse layer	Bone	6563	44	0	6563	2,8		R_Date("64", 6563, 44){z=-2.80;color="grey"};
6264786,95	600037,99	AAR-13395	65	Jesholm 1, coastal settlement, fireplace	Wood, Charcoal	6980	48	0	6980	2,35		R_Date("65", 6980, 48){z=-2.35;color="green"};
6260144,23	663655,46	AAR-4061	66	Kattegat, core no. 572011	Marine shells, *Cerastoderma edule, Macoma balthica*	9235	55	400	8835	-30,2		R_Date("66", 8835, 55){z=-30.20;color="blue"};
6260098,90	664351,85	AAR-4062	67	Kattegat, core no. 572012	Marine shells, *Balanus crenatus, Cerastoderma edule*	8520	55	400	8120	-28,7		R_Date("67", 8120, 55){z=-28.70;color="blue"};
6260098,90	664351,85	AAR-4063	68	Kattegat, core no. 572012	Marine shells, *Cerastoderma edule*	9145	75	400	8745	-33,35		R_Date("68", 8745, 75){z=-33.35;color="blue"};
6241834,11	634629,94	AAR-4529	69	Kattegat, marine shells	Marine shells, *Macoma baltica*	8760	75	400	8360	-29		R_Date("69", 8360, 75){z=-29.00;color="blue"};
6242648,13	635456,57	AAR-4530	70	Kattegat,	Marine shells, *Mytilus edulis*	8790	75	400	8390	39,5		R_Date("70", 8390, 75){z=-39.50;color="blue"};